Combination of Extracorporeal Shock Wave Therapy and Low Intensity Ultrasound for Inducing Healing of Non-union in a Rabbit Model

Hui Chi Cheung

Dissertation submitted for the degree of
Master of Philosophy
in Rehabilitation Science

Department of Rehabilitation Science
The Hong Kong Polytechnic University
April 2004

Statement of Sources

The idea of the present investigations and planning of the experiments resulted from the discussions between the author, Dr. Xia Guo and Dr. Kevin Kwong.

All experiments in the present investigation were completed solely by the author.

The author declares that the work presented in the thesis is, to the best of the author's knowledge and belief, original, except as acknowledged in the text, and that the material has not been submitted, either in whole or in part, for a degree at this or any other University.

Benny C. C. Hui (BScPT)

April 2004

Acknowledgements

I wish to thank the colleague in the Department of Orthopedics and Traumatology of the Chinese University of Hong Kong, for their support of space and facilities in developing and completing this study. I wish to thank Mr. Francis Chan for the technical support and his valuable advice and contribution to the study, as well as Mr. Benson Yeung and the orthopedic research team working in the Lee Hysan Clinical Research Laboratory of the Princess of Wales Hospital for their help in conducting the experiments.

I have to special thanks to the persons who worked closely with me and the research staff in the Department of Rehabilitation Science of the Hong Kong Polytechnic University. I am not able to handle the huge amount of daily research work and dedicated in my postgraduate school life without their helping hands.

However, my most intimate acknowledgements are for Dr. Xia Guo and Dr. Kevin Kwong, my supervisors, who kindly and strongly supported my work and my personal growth, and also my family's support to my commitment of the study.

This research project is supported by AO Research Grant 02-G4.

Abstract

Introduction: Despite the advances in modern orthopedic fracture treatment, the rate of delayed union or non-union in all types of fractures remains about 10%. Most recently, two biophysical methods, extracorporeal shock waves (ESW) and low intensity pulsed ultrasound (LIPU), have been shown to be effective in healing fracture non-union. It is suggested that, single ESW treatment could be a trigger that can "initiate" the ossification procedure in the non-union site. On the contrast, LIPU therapy requires daily application over a time period of months to enhance repair process. Objectives of this study were: (1) to compare the success rate, healing quality of a non-union among 3 treatment methods of isolated ESW, LIPU and combined therapy; (2) to investigate the pattern of healing to non-union by the 3 different methods.

Methods: New Zealand White rabbit of 18 weeks (about 3kg) was used in the study. With 24 rabbits performed right tibia osteotomy, they were equally divided into four groups at post-operation week 12: the control group, ESW treatment group, LIPU treatment group and the ESW plus daily LIPU treatment group. Radiographs were taken for all groups postoperatively week 12, 14 and then biweekly until week 22. Rabbits were sacrificed postoperatively at week 22 for evaluations of repair using peripheral quantitative computerized tomography (pQCT), microcomputerized tomography, fluorescence microscopy and light microscopy.

Results: The union rate in isolated ESW and LIPU group were both 66.7%, as well as the combined treatment was 66.7%, while there was no single union case formed in the control group at week 22. The difference was of statistic significance ($p<0.05$). Fluorescence microscopic findings suggested that 3 treatment methods promoted bony bridging mainly by endochondral bone formation in the non-union gap, without obvious periosteal callus formation. The healing pattern of LIPU and combined treatment was similar with slower onset of new bone formation than ESW but the healing quality was better and bone cell density was higher than ESW group at week 22 in microscopic evaluations.

Conclusion: ESW, LIPU and combined treatment were effective to the healing of non-union. The pattern and the process of ESW promoted bony bridging in fracture non-union were distinct from those found in typical primary or secondary fracture healing. Similar pattern was also revealed in the combined treatment and LIPU treatment groups.

Table of Contents

List of Tables

List of Figures

List of Appendices

Chapter 1: Introduction

1.1. Background of the study

Non-union of a fracture is diagnosed if it can be determined clinically or radiographically that healing has ceased and healing is highly improbable. Treatments of fracture non-union aim at re-activating the normal fracture healing process. The primary choice in clinical practice is surgical methods. Although the success rate of surgical treatment is reported as being up to between 86% to 93% [2, 41, 58], complications from surgery, such as surgical infection, failure of fixator and damage to the surrounding nerves and blood vessels[47], need to be borne in mind.

As a result, it is important to develop an effective non-operative therapy for fracture non-unions. Low intensity pulsed ultrasound (LIPU) and extracorporeal shock waves (ESW) have been shown to be effective in healing fracture non-unions [25, 26, 34, 44]. It is suggested that ESW could be a trigger in initiating the ossification process at the non-union site. A single application of ESW has been demonstrated to result, several months later, in bony consolidation of the non-union [44]. In contrast, LIPU therapy requires daily application over several months [34]. This suggests that the role LIPU plays in non-union healing tends more toward sustaining and enhancing the progress of ossification.

The comparison of the characteristics of ESW and LIPU therapy for non-union is illustrated in Table 1. It has been demonstrated that healing of non-union can be achieved with ESW therapy within a relatively shorter period (average healing time 3.4 months) but with a relatively lower success rate (around 60%) [57]. LIPU therapy has the reverse effect, i.e. a higher success rate (90%), but requiring a longer duration (average healing time more than 5 months) [29].

Table 1.1a: Comparison of ESW and LIPU therapy for non-union

	ESW	**LIPU**
Application mode	Single application	Daily application for months
Average healing time	3.4 months	152 days (5 months)
Success rate	60%	90%

1.2. Animal non-union model

A number of previous studies have reported methods for the creation of animal non-union models. Brownlow and Simpson [6] created a rabbit tibia defect non-union model. Adult female New Zealand White rabbits were used. Operations were performed under general anesthesia and aseptic conditions. Osteotomy was done at the midshaft of the tibia and was fixed with an external fixator. A 2 mm gap was introduced immediately with clearing of the periosteum and the content of the intramedullary canal. Their results showed a non-union rate of over 90%, with little callus formation and the growth of fibrous tissue inside the gap [6]. Oni and Rompe [40, 45] also created a reproducible rabbit defect non-union model using a similar procedure. In addition to the rabbit model, dog and rat models have also been described [14, 26].

However, there have been relatively few papers which used an animal model to study the effect of ESW. Johannes et al chose the dog radius non-union model and a single application of 1,000 ESW pulses at 0.54 mJ/mm^2 [26]. They reported that there were immediate non-detectable changes at post-treatment, signs of bridging callus at week 6 and completed bony union at week 12. Histology revealed that there was bony union on both the periosteal and endosteal sides [26]. However, the study failed to provide information on the histology immediately after ESW to permit investigation on how the treatment can induce fracture healing of non-unions.

Another animal study was used to test the application of LIPU to the healing of non-unions. Takikawa created a rat tibia non-model and treated it with a daily application of LIPU [53]. The parameter settings of the ultrasound treatment were: 200 ms burst sine wave, 1.5 MHz frequency, at an intensity of 30 mW/cm^2. They reported that endochondral bone formation was observed after 4 weeks of treatment. Fracture callus and a decrease in the fracture line were found at week 6 of treatment. The mechanism which they proposed was the possible exertion by LIPU of a mechanical force on the cells in the soft tissue at the fracture gap. The fibrous tissue at the non-union site was stimulated by LIPU, inducing the cells to differentiate into chondrocytes and leading to endochondral ossification and bone union [53].

1.3. Application of ESW to the treatment of non-union

In clinical practice, shockwaves were originally applied in lithotripsy, to break up and destroy stones in the renal, biliary and salivary gland tracts [44]. A shock wave is defined as an acoustic wave the pressure of which rises from the ambient value to the maximum value within a few nanoseconds [46]. The typical form of a shock wave is a sharp positive rise in pressure in nanoseconds followed by a gentle and variable negative pressure over microseconds (Fig. 1.2a) [38].

The focal area is defined as the area in which 80% of the maximum energy is reached [27]. The term energy flux density is used to describe the shock wave energy flows through an area perpendicular to the direction of propagation [46]. It can be expressed in the following formula (and is measured in millijoule/millimeter^2 (mJ/mm^2) units).

Energy Flux Density = dE / dA

E – energy of shock wave at particular location

A – area in which the shock wave is existent

According to Rompe, the energy levels can be divided into low, medium and high [45]. Shock waves of different energy levels will cause different effects inside the body. They are summarized in figure 1.2b.

Cavitation is the effect of the occurrence of gas bubble filled hollow bodies in a liquid medium. In stable cavitation, the bubbles are in equilibrium when the vapor pressure inside the bubble is equal to the external pressure of the liquid [46]. When a shock wave hits the bubble, the peak rising energy will cause the collapse of the bubble within 2-3 microseconds. The gentle negative pressure energy of the shock wave will cause bubbles to grow significantly, reaching as much a 10^9 of their original size. This will cause the destruction of the material because its tensile strength is exceeded due to the pressure change [46].

The body includes various tissues which have different degrees of elasticity and compressibility, and affect the propagation speed of sonic waves. When a shockwave enters the body, transmission through and reflection from different media occurs due to their different acoustic impedance: (water 1.49; muscle 1.72; fat 1.37; cortical bone 7.38; renal stone 6.25) [38]. As cortical bone and renal stone have similarly high acoustic impedance values, it is believed that shockwaves cause microfractures to bone which are similar to the disintegration of renal stones. Ogden et al [38] reported that the intensity of a shockwave transmitted into cortical bone is about 65% of incident intensity, causing a strong interaction at the periosteal interface. The cavitation effect also causes partial osteocyte death, followed by the migration of osteoblasts to the non-union site for local new bone formation [38].

The effectiveness of ESW on healing non-unions has been demonstrated in some clinical studies. Wang et al [59] reported a success rate of 80% in 12 months with the

application of 6,000 impulses at 28 kV to hypertrophic non-unions. Schaden et al [49] reported a healing rate of 75.7% in 18 months following 12,000 impulses at 28kV. Rompe et al also reported that 72% of patients showed bony consolidation after a single shockwave treatment [47]. None of the studies showed any discernable side effects after shockwave treatment.

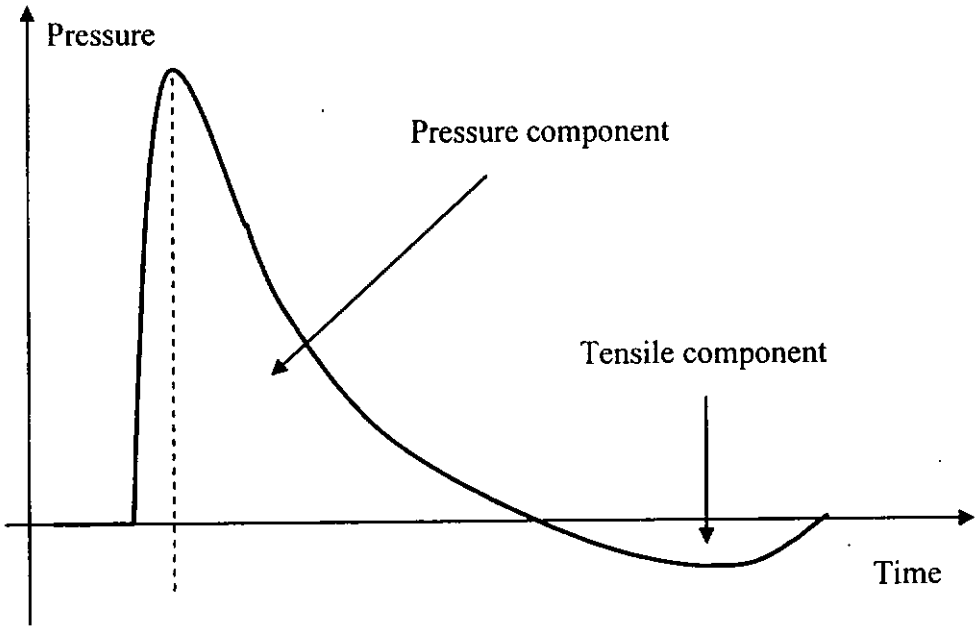

Fig 1.3a. Typical form of shockwave

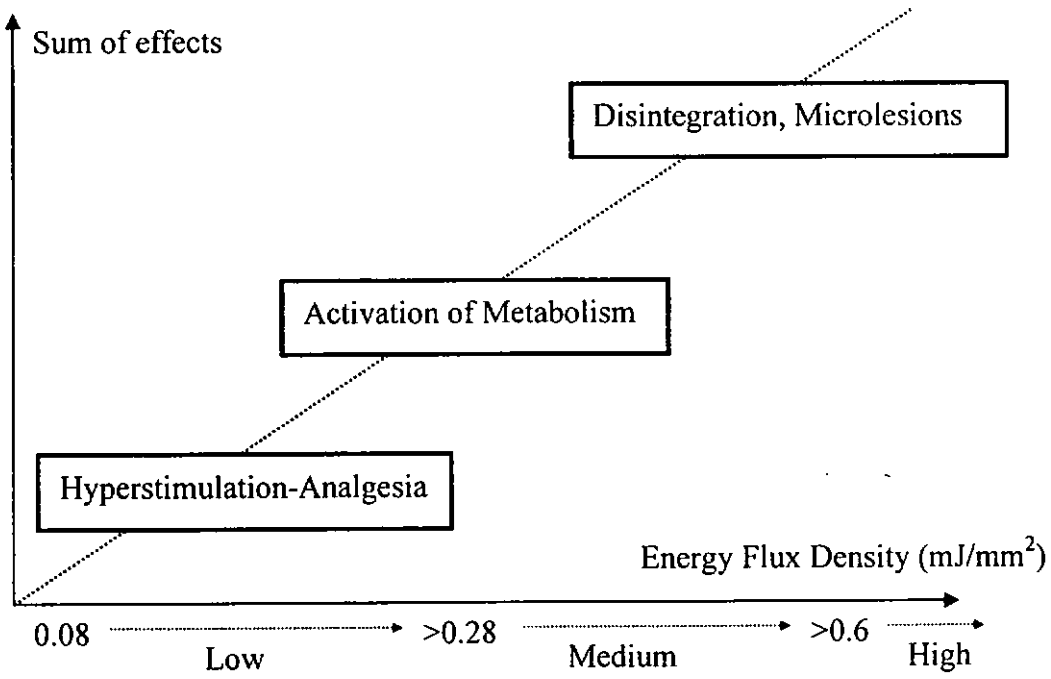

Fig 1.3b. Biologic effect of shockwaves at different energy level

1.4. Application of LIPU to the treatment of non-union

Ultrasound is a type of acoustical pressure wave with a frequency above the audible sound range (>20kHz). Continuous ultrasound is a sine wave with a specific frequency and amplitude (Fig. 1.4a). Pulsed ultrasound has its intensity periodically interrupted by an interval during which no ultrasound energy is produced, its average energy thus being reduced. The intensity of an ultrasound is a measure of the rate at which energy is delivered per unit area, and measured in units of milliwatt per unit square (mW/cm^2) [62].

The physiological effects of ultrasound include thermal and non-thermal effects. The thermal effect of ultrasound can cause a rise in tissue temperature, continuous waves more so than pulsed waves. The non-thermal effects include cavitation and acoustic streaming. Both will cause the unidirectional movement of fluid along the boundaries of cell membranes, altering their function and structure without damaging the cell [62].

Low intensity pulsed ultrasound (LIPU) has been shown to accelerate the healing of fresh fractures both clinically and experimentally. Clinical studies on the influence of LIPU in fresh tibial diaphysis fractures demonstrate a significant acceleration of 38% in the time required for a fracture to heal, from 154 to 196 days [24]. Similar results were reported for distal radius metaphyseal fractures, with a significant 38% acceleration in the LIPU-treated group whose fractures healed in 61 days as compared with the un-treated group's average healing time of 98 days [26]. Recently, several studies have further

demonstrated the effects of LIPU in the successful treatment of delayed unions and non-unions [24, 28, 34]. Mayr et al reported the use of LIPU in the therapy of 951 delayed unions and 366 non-unions [34]. The overall success rate for delayed unions was 91%, with an average healing time of 129 days, and that for non-unions 86%, with an average healing time of 152 days.

The exact mechanism by which ultrasound affects the healing of fresh fractures and of non-unions is still under investigation. Studies investigating the biological effects of ultrasound on bone suggest that it has a direct mechanical effect on cell proliferation. Ultrasound also affects cell function. In vitro, ultrasound can induce a significant increase of calcium absorption in isolated mesenchymal cells as well as in cartilage cells [41].

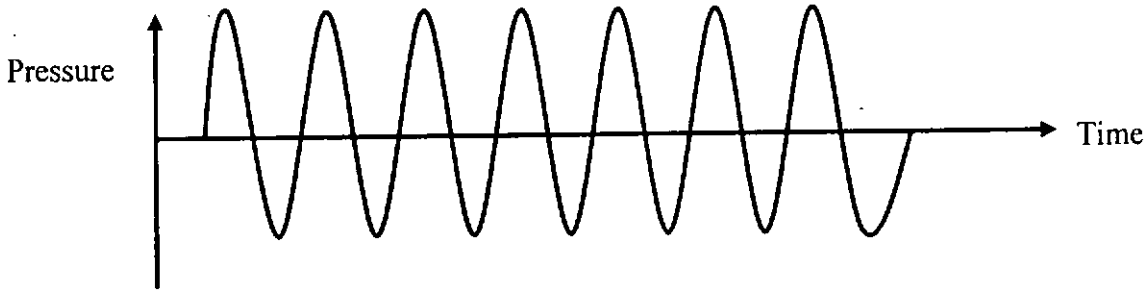

Fig 1.4a. Typical form of ultrasound wave

1.5. Objectives of the study

Both the healing of fresh fractures and ESW-induced healing of non-unions occur through callus formation. We postulate that the application of LIPU can enhance ESW-induced callus formation in a way similar to its effects on the healing of fresh fractures. A combined application of ESW and LIPU therapy may thus achieve a more optimal healing of non-unions than using either method alone. This could eventually result in shortening the duration of non-union healing and increasing the healing success rate.

The effectiveness of the treatment was estimated by comparing the success rate, healing quality and healing time of non-unions. The objectives of the study are set forth below.

1. To evaluate the effect of ESW on non-unions
2. To evaluate the effect of LIPU on non-unions
3. To evaluate the effect of a combined treatment
4. To investigate the pattern of induced healing by above 3 interventions

Chapter 2: Methodology

The following experiments were conducted after receiving ethics approval from the Animal Research Ethics Committee of the Hong Kong Polytechnic University (PolyU) and the Chinese University of Hong Kong (CUHK) (Appendix 9).

2.1. Animals

Twenty-four mature Female New Zealand White rabbits of 18 weeks of age with an average body weight of 3.2 kg (2.7-3.8 kg) were used. The rabbits were kept in individual metal cages in CUHK central animal house and supplied with standard rabbit food and water *ad libitum*. They were housed in individual cages in rooms controlled for temperature (23°C) and humidity (50%) that had an 8-hour light / 16-hour dark cycle, with lighting on from 9am to 5pm every day.

2.2. Design of the experiment

A non-union was created in the midshaft of the right tibia of each rabbit through osteotomy and external fixation for 12 weeks.

At the end of week 12 post-operation, a successful tibia non-union with persistent fracture gap, absence of bridging callus and presence of sclerotic bone ends was confirmed radiographically. The 24 rabbits were randomly divided into four groups. The control group (Group I) did not receive any treatment; the ESW group (Group II) received a single application of ESW therapy on the 1st day (post-op week 13) after the diagnosis of non-union; the LIPU group (Group III) was treated with LIPU daily from the second day after the diagnosis to the end of the experiment; and the combined treatment group (Group IV) was treated with ESW on the first day, followed by a daily LIPU treatment from the second day after the diagnosis of non-union.

In vivo follow up of bony changes in the treatment area was documented by antero-posterior (AP) plain X-ray. Sequential fluorescent labeling of new bone formation was performed. Following the procedure applied by Rompe, 90 mg/kg of xylenol orange and 20 mg/kg of Calcein green were used [46]. Calcein green was injected at post-op week 12 and 14 and xylenol orange was injected at week 16, 18, 20 to detect the new bone formation in the above time intervals. Each group of animals was euthanized at week 22. After the animals were euthanized, the bilateral tibiae were harvested and fixed in buffered formalin. Peripheral quantitative computerized tomography (pQCT) was used to

measure the bone density of the bilateral tibiae. The non-union site of the right tibiae was harvested for histomorphological analysis.

The total sample size in this study was set at 24, with 6 animals per group. The number of animals would be added in case that there was no any significant results obtained (Union score, BMC) after data analysis.

2.3. Non-union model

The right tibia was shaved up to mid-femur level. General anesthesia with sodium pentobarbital (Sigma, Chemicals Co., St. Louis MO, USA) was applied in a dosage of 0.8 ml/kg by intra-venous mode. The rabbit was checked for full anesthesia by testing the eye-lip reflex and the relaxed breathing pattern. The limb was wrapped with sterile cloth leaving the tibia exposed. An incision was made along the tibia using the medial approach. The periosteum was separated carefully from the surrounding muscles. Four holes were drilled using an electrical drill bit with a shaft diameter of 2.5 mm, spaced in conformity with the position of the holes of the external fixator. Four self-drilling mini cortical screws (Orthofix, Italy) with a shaft diameter of 2.5-3 mm and a thread length of 18 mm were inserted into the tibia. After the screws were inserted, a 5 mm bone defect located about 12 mm proximal to the tibial tuberosity was created by using an oscillating saw powered by an air power drill. The saw blade was 0.4 mm in thickness (Synthes, Mathys AG, Bettlach, Switzerland). 5 mm of the periosteum was stripped off, and 5 mm of the intramedullary canal was curetted. The surgical site was cleaned and irrigated using a sterile saline. The defect was left empty and a stainless-steel external fixator (modified from Orthofix M103) was used for bony fixation. The surgical incision was closed by suture (3/0 Mersilk, Ethicon Ltd. Edinburgh, Scotland). An antibiotic spray (Nebactin, Byk Gulden Konstanz, Germany) was used for disinfection. A post-op radiograph was taken immediately after the surgery. The animals were allowed free activity in their cages immediately after the operation.

Some rabbits were found to have small bone cracks during the course of drilling the holes and osteotomy. In these cases, K-wires were used to fix the cracks by winding the wire around the circumference of the tibia. The operation procedure is shown in Figure 2.3a-2.3e. The detailed operation protocol is shown in appendix 1.

The rabbits were cared for a period of 12 weeks after the operation. The treatment was started on the rabbits whose non-union conditions were confirmed.

Fig 2.3a. Medial incision of the tibia

Fig 2.3b. Two out of four screws inserted in the medial side of tibia

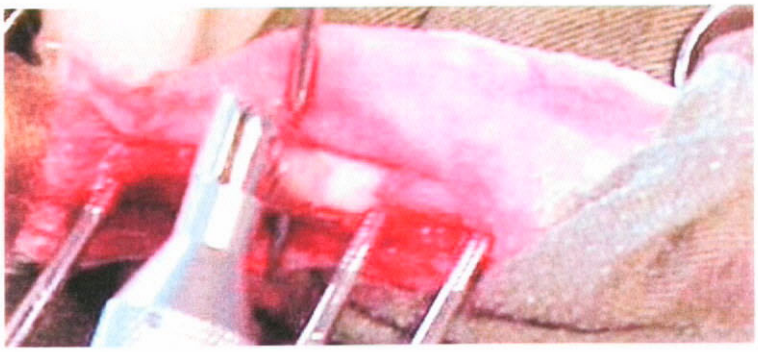

Fig 2.3c. Air power saw for creating osteotomy

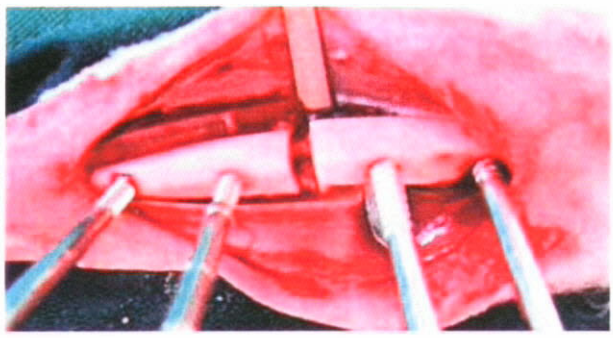

Fig 2.3d. Periosteum and intramedullary nail removed

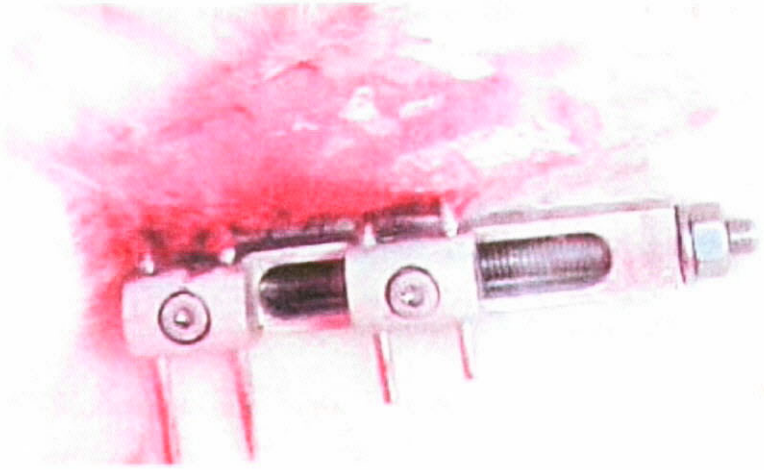

Fig 2.3e. Fixator applied and wound closed by suture

2.4. Biophysical interventions at the non-union site

2.4.1. Anesthesia

Anesthesia for daily LIPU and for the ESW treatment was administered at a dose of 1.5 ml/kg through an intra-muscular (IM) injection. The anesthetic solution combined 0.6 ml of 10% ketamine hydrochloride (Alfasan, Woderden, Holland) and 0.9 ml of 2% xylazine hydrochloride (Alfasan, Woderden, Holland). A 25 gauge needle was used for the IM injection.

2.4.2. Extracorporeal Shockwave (ESW) treatment

The animals in the ESW group received a single application of ESW on the 1st day of post-op week 12. A SONOCUR Plus (Siemens, Erlangen, Germany) shock wave generator located in the physiotherapy clinic of the university was used in the study. Before the treatment, the rabbits were sedated by anesthesia with a mixture of 0.9ml xylazine and 0.6ml ketamine. The hair was shaved at the treatment site. 70% ethanol was used to clean the sound head before and after treatment. The rabbits were positioned on the bench in such a way as to keep the non-union site at the center of the focus during the application of ESW therapy (Fig. 2.4a). Transmission gel (Chattanooga Group Inc, TN, USA) was used as a coupling medium between the shock wave generator and skin. One thousand shock waves at a power setting of 0.54 mJ/mm^2 were applied to the non-union site. The total treatment time was 10 minutes. Redness of the skin was observed after the treatment, which gradually returned to normal after 4-7 days. The detailed protocol is shown in appendix 2.

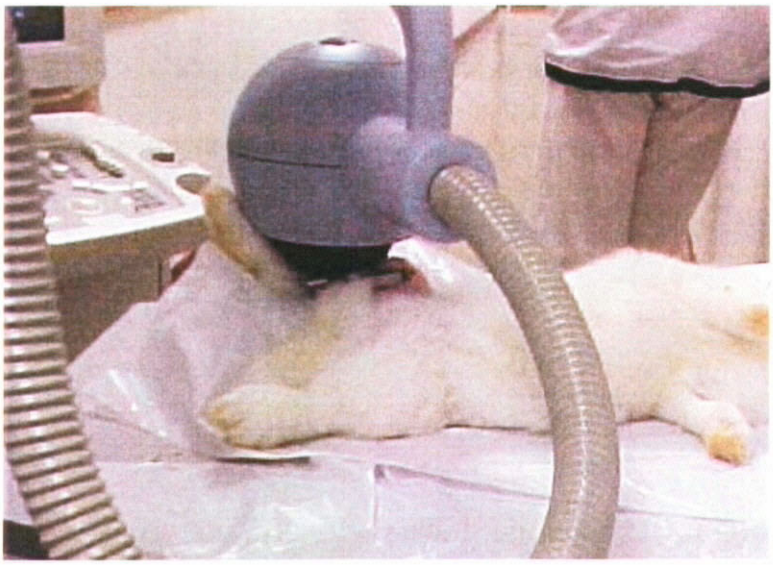

Fig. 2.4a. ESW application to rabbit tibia

2.4.3. Low intensity pulsed ultrasound (LIPU) treatment

LIPU was delivered by a 2.5 cm diameter ultrasound transducer (SAFHS, Exogen, Inc, West Calwell, NJ, USA) placed against the anterior surface of the non-union site. The signal was applied in a burst rather than continuously to obtain a ratio between peak amplitude and average power so as to avoid cavitation and tissue heating. The output of the ultrasound machine was tested using the SAFHS light indicator at weekly intervals. The rabbit was sedated using the same anesthesia as that used in ESW treatment and ultrasound transmission gel was applied. LIPU treatment lasted for 20 minutes, 6 days per week for a total of 10 weeks. The machine settings are shown in table 2.4a. The detailed protocol is shown in appendix 3.

Table 2.4a: Characteristics of low intensity pulsed ultrasound (LIPU) (manual of SAFHS, Exogen, Inc, West Calwell, NJ, USA)

Frequency:	1.5 MHz	**Off period:**	800 s
Wave shape:	Sine wave	**Repetition rate:**	1 kHz
Signal type:	Pulsed	**Intensity:**	30 mW/cm^2
Length of signal:	200 s		

2.5. Outcome evaluation

2.5.1. Radiographical evaluation

A plain X-ray was taken biweekly (in week 12, 14, 16, 18, 20 and 22). An anterior-posterior (AP) radiograph of the operated limb was taken using a Faxitron X-ray machine (Model 43855C, Wheeling, IL, USA) at a setting of 60 kV for 5 seconds. The positioning of the rabbit is shown in the figure 2.5a. A medio-lateral image was not possible due to the presence of the stainless steel fixator at the non-union site. The films were processed using an automatic X-ray developer (Okamoto X3, Okamoto manufacturing Co. Ltd., Taiwan). The union rate and union score were calculated at the end of the experiment.

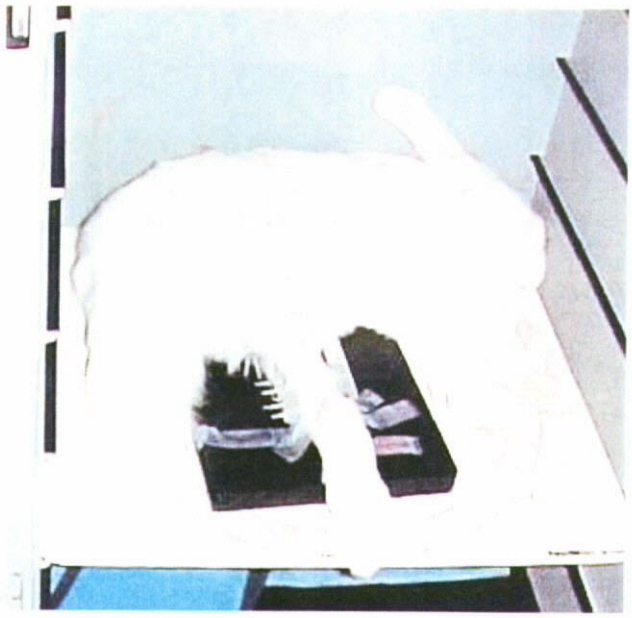

Fig 2.5a. Positioning of rabbit in the x-ray chamber of Faxitron x-ray machine (Model 43855C)

2.5.2. pQCT measurement

A pQCT (XCT 2000, Stratec, Germany) was used to scan and quantify volumetric bone mineral density. The machine produces a narrow beam of X-rays operating at 60 kV. The detector system consists of 12 cadmium telluride detectors assembled in line. The diameter of the central circle is 150 mm. The scanner's performance was evaluated by different phantom experiments. The calibrations were done by standard phantom at 5-day intervals, and cone phantom at 25-day intervals. The tibiae were divided into three groups for measurement: proximal cortex, gap and distal cortex. A 2 mm length was taken from each group for analysis through two consecutive transverse pQCT scans of a thickness of 1 mm.

The tibia of a euthanized rabbit was removed and wrapped in a plastic bag during pQCT scanning. The setup position is shown in figure 2.5b.

The data was analyzed using the machine's software (Version 5.50B, Stratec Medizintechnik GmbH). The detailed procedure is reported in Appendix 7.

Fig 2.5b. Set up position for pQCT measurement of the fracture gap

2.5.3. Polychrome fluorescent sequential labeling

Polychrome sequential labeling was introduced by subcutaneous injection with 2 different dyes, calcein green and xylenol orange. The bone formation dynamic was viewed under fluorescence microscopy on undecalcified bone sections.

A calcein green (Sigma-Aldrich, St. Louis, MO, USA) dosage of 10 mg/kg was used. The solution was prepared by dissolving 1 g of calcein green powder in 80 ml distilled water. It was stirred and its pH value adjusted to 7.2-7.4 by adding drops of NaOH solution using a pH meter. After all of the powder had dissolved, distilled water was added up to 100 ml and stored away from sunlight. 3 ml of the calcein green solution were injected on each occasion.

For xylenol orange (Sigma-Aldrich, St. Louis, MO, USA), the dosage was 90 mg/kg. The solution was prepared by adding 9 g of xylenol orange powder to 80 ml of distilled water. It was stirred and its pH was adjusted to 7.2-7.4 by adding drops of NaOH solution using a pH meter. After all of the powder had dissolved, distilled water was added to 100 ml and stored away from sunlight. 3 ml of the xylenol orange solution were injected on each occasion.

Calcein green was injected on the first day and at the second week after treatment (post-op week 12, 14) and xylenol orange was injected at the fourth week, sixth week and eighth week (post-op week 16, 18, 20) to label the time and site of new bone formation.

These dyes can be incorporated into the newly formed bone during the mineralization phase of the newly formed bone matrix. Under fluorescence microscopy using a blue filter (wavelength 400-700 nm), the two dyes emit a green and orange fluorescence respectively, giving a reliable estimate of the location of new bone formation at different points in time.

2.6. Tissue processing for histomorphometry

2.6.1. Euthanasia

Six animals from each group were euthanized in week 22 after surgery. With the rabbits sedated using a mixture of 0.9 ml of xylazine and 0.6 ml of ketamine (intra-muscular injection), a 23 gauge catheter was inserted into the marginal ear vein. 1 ml of 25% sodium pentobarbital was injected intra-venously and the animal was euthanized using an over-dose of anesthesia.

2.6.2. Tissue harvesting

The bilateral tibiae were harvested with incision through the knee and ankle joints. The skin was removed and most of the surrounding muscle retained. A pair of specimens was placed in 10% neutral buffered formalin at room temperature for one day, and then changed to 70% ethanol for storage at room temperature.

After completion of pQCT measurement, the central part of the right tibia was removed using an oscillating saw for further histological processing. The site of the selected sample was at the position proximally just below the second pin and distally just above the third pin. A horizontal line was sawn in the proximal position and an oblique line was sawn in the distal position of the sample, with the medial part higher than the lateral part, at an angle of around 20-30 degrees. The purpose was to identify the orientation of the sample when sectioning and performing microscopic analysis at a later stage.

A decalcified histology was performed on one specimen from each group. The samples were stored in 9% formic acid at room temperature for one month. The solution was changed weekly to ensure effective decalcification. Decalcification was completed in one month time and the samples were tested by cutting with a microtome knife. They were embedded in paraffin and serial sagittal sections of a thickness of 6 μm were cut using a microtome (RM2165, Leica Instruments, Nussloch, Germany). Sections were stained with hematoxylin and eosin (H & E) in accordance with the protocol described in Appendix 5 [30]. Microscopic photos of each section were taken using both 1.6x and 10x magnification.

The density of osteocytes in the 4 H&E stained samples were evaluated using the 10x magnification photos. 3 randomly selected sites were chosen from each section and the number of osteocytes was marked manually in a fixed 400x400 pixel grid for the comparison of cell density with other samples.

2.6.3. 3D Microcomputerized tomography

Four rabbit tibia samples chosen from each group for microcomputerized tomography (μCT) measurements were first embedded in methyl methacrylate (MMA). A μCT-40 scanner (Scanco Medical, Zurich, Switzerland) was used for scanning. Resolution was set at 36 μm and a total of about 240 slices were taken from the treatment site, commencing approximately 5mm above and ending approximately 5mm below the observable site of the gap (Fig. 2.6a). With the analysis software, both the cortical and trabecular structures of each sample were captured for qualitative analysis.

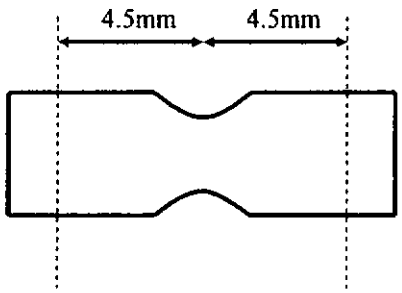

Fig 2.6a. Graphical representation range of μCT scanning

After scanning, all the 240 2D slices were taken and combined for 3D quantification. 3D reconstruction of the image was performed by the software and the positions of both the cortical and trabecular structures were captured for each sample to illustrate the characteristics in each of the different groups.

2.6.4. MMA Embedding

The samples were fixed and dehydrated in a series of graded ethanol (70%, 80%, 90%, 100%), and embedded undecalcified in methyl methacrylate (MMA). The detailed protocol for embedding is described in Appendix 6 [20].

2.6.5. Histomorphometry

The MMA embedded samples were sectioned by a saw microtome used for hard tissue (SP 1600 Leica, Germany) to a thickness of 100 μm. Microradiographs of each bone section were taken by a Faxitron radiograph machine (Model 43855C Wheeling, IL, USA), using high resolution X-ray film (Structurix D4 Pb Vacupac, Agfa, Japan). The exposure conditions were: 45 kV, 2 mAs, with a X-ray source to object distance of 40 cm. One of the MMA sections representing the central bone section including the proximal cortex, gap and distal cortex of the tibia was chosen and observed on the microradiograph. Super-glue was used to mount the section onto the acrylic slide. The section was polished using a grinding machine (Struers Rotopol-21, Rodovre, Denmark) and viewed under fluorescence microscopy. Histomorphometric analysis was performed by viewing the fluorescent section at 1.6x magnification, to assure visualization of the non-union area. The image was then captured using a digital camera attached to the microscope and displayed on the computer monitor (Leica image analysis system Q500M). The quantification was performed using the image analysis software (ImageJ 1.29x, Wayne Rasband, National Institutes of Health, USA). The area of mineralization was traced and

measured using pixels as the unit. The areas of the green dye and orange dye were auto-detected and counted as a percentage of the total area.

Another 4 decalcified sections embedded in paraffin were cut to a thickness of about 6 μm by saw microtome. The sections were stained with Haematoxylin & Eosin (H & E) to demonstrate the union status and the density of the mature osteocytes. Microscopic photos of each sample were taken at magnifications of 1.6x and 10x. The ImageJ software (ImageJ 1.29x, Wayne Rasband, National Institutes of Health, USA) was used for quantification of the number of cells in the 10x magnification photos. The total image size was set at 1,300 × 1,030 pixels. Inside the photo, 3 random sites of 400 × 400 pixels were chosen and the number of cells counted manually for comparison of the cell density among the samples with different treatments.

2.7. Data Analysis

Testing for differences among the 4 groups was performed. The union rate, union score and BMC data were analyzed using One-Way Analysis of Variance. The statistical significance level was set at a probability of less than 0.05. If any significant effect was found, a post hoc Tukey multiple comparisons test was performed to test for the mean differences among the 4 groups using pairwise comparisons. SPSS 11.0 was used for the statistical analysis.

Chapter 3: Results

3.1. Radiographic Findings

The serial radiographs provided the means of observing the progress of healing at the non-union site for the different treatments. For each animal, the union was classified into one of four categories and scored as follows:

Score	Radiographic evidence
3 =	**Union:** bony bridging between the bone ends
2 =	**Partial union:** positive bony reaction, but bony bridging occured only at selected points
1 =	**Uncertain:** the bone ends contact with each other without new bone formation at the non-union site
0 =	**Non-union:** clear non-union gap

The union rate was calculated using the following formula:

Union rate (%) = (number of unions / group size) × 100%

3.1.1. Union rate

By week 22, all 6 rabbits in the control group showed a persistent fracture line at the non-union site, with a sclerotic bone end at the proximal and distal segments of the fracture. The non-union gap was in irregular shape and varied in width from 0 to 2.0 mm. In the ESW therapy group, gradual new bone formation in the non-union gap was observed in all 6 rabbits. At the end of the experiment, full bony bridging of the non-union gap was observed in 4 out of 6 rabbits and partial bony bridging in the other 2. In the daily LIPU treatment group, 4 complete unions, 1 partial union and 1 sample without any evidence of union were observed after 10 weeks of treatment. In the combined ESW and LIPU treatment group, there were 4 complete unions and 2 partial unions. The healing curve of non-unions is presented in figure 3.1a. By the end of the experiment, the union rate was 0% in the control group and 67% in the ESW, LIPU and combined treatment groups. One-way ANOVA showed a significant difference in the union rate between the control group and each of the treatment groups ($p<0.05$), whereas there was no significant difference among the 3 different treatment groups.

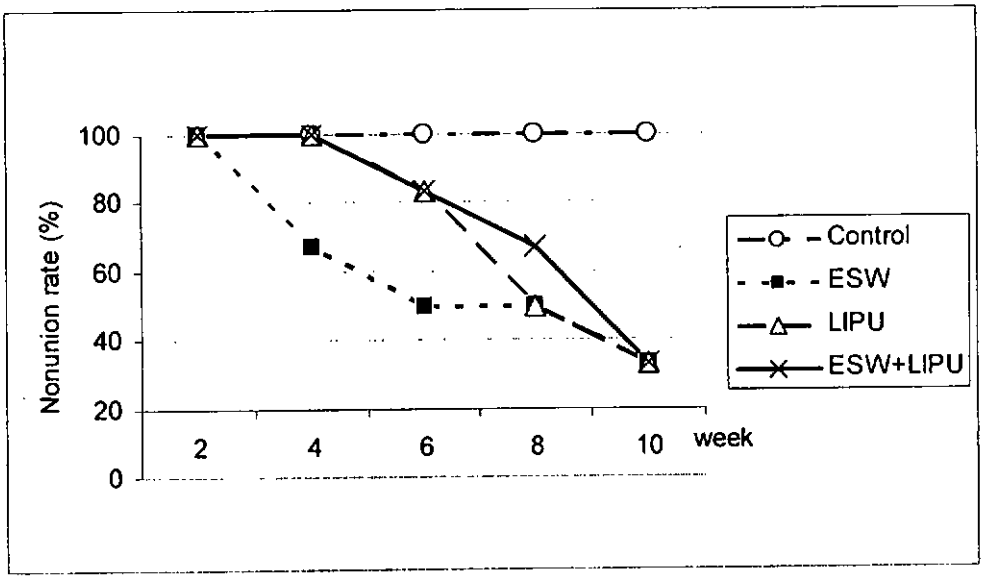

Fig 3.1a. Decrease in non-unions over time after different treatments

3.1.2. Union score

There was a similar pattern of bony bridging of the non-union gap in the 3 treatment groups. There was gradual mineralization and an increase in bone mineral density (BMD) during the initial four weeks of treatment. After that, bone formation ceased in some cases, resulting in partial unions 10 weeks after treatment, while in other cases, there was continuous active bone formation until the end of the experiment, resulting in complete unions. The progress of healing following each treatment is demonstrated in figures 3.1b, 3.1c, 3.1d and 3.1e and was measured quantitatively by the union scores as summarized in tables 3.1a, 3.1b, 3.1c and 3.1d. Table 3.1e compares the union rates and scores among the 4 groups.

Union scores increased with time in all groups, with the exception of the control group. By the end of the experiment, the mean union score was 0.5 ± 0.22, 2.5 ± 0.34, 2.33 ± 0.49 and 2.14 ± 0.46 in the control group, ESW group, LIPU group and combined treatment group respectively. A nonparametric test showed a statistically significant difference in the union scores between the control group and those of other three treatment groups ($p<0.05$), but no significant difference among the three treatment groups (Fig 3.1f).

Table 3.1a. Radiographic evaluation of number of healing cases in fracture non-union over time in control group (n = 6)

Union score	Week 2	Week 4	Week 6	Week 8	Week 10
3 (n =)	0	0	0	0	0
2 (n =)	0	0	0	0	0
1 (n =)	4	4	4	4	4
0 (n =)	2	2	2	2	2
Total score*	4	4	4	4	4

*Total score = Σ (union score x n)

Table 3.1b. Radiographic evaluation of number of healing cases in fracture non-union over time in ESW group (n = 6)

Union score	Week 2	Week 4	Week 6	Week 8	Week 10
3 (n =)	0	2	3	3	4
2 (n =)	3	1	1	2	1
1 (n =)	2	3	2	1	1
0 (n =)	1	0	0	0	0
Total score*	8	11	13	14	15

*Total score = Σ (union score x n)

Table 3.1c. Radiographic evaluation of number of healing cases in fracture non-union over time in LIPU group (n = 6)

Union score	Week 2	Week 4	Week 6	Week 8	Week 10
3 (n =)	0	0	1	3	4
2 (n =)	3	3	3	2	1
1 (n =)	1	2	1	0	0
0 (n =)	2	1	1	1	1
Total score*	7	8	10	13	14

*Total score = Σ (union score x n)

Table 3.1d. Radiographic evaluation of number of healing cases in fracture non-union over time in ESW+LIPU group (n = 6)

Union score	Week 2	Week 4	Week 6	Week 8	Week 10
3 (n =)	0	0	1	2	4
2 (n =)	1	2	4	3	1
1 (n =)	4	3	1	1	1
0 (n =)	1	1	0	0	0
Total score*	6	7	12	13	15

*Total score = Σ (union score x n)

Table 3.1e. Comparison of union rates and total union scores among the 4 groups (n = 6)

	Week 2		Week 4		Week 6		Week 8		Week 10	
	rate[1]	score[2]	rate	score	rate	score	rate	score	rate	score
Group 1	0%	4	0%	4	0%	4	0%	4	0%	4
Group 2	0%	8	33%	11	50%	13	50%	14	67%	15
Group 3	0%	7	0%	8	17%	10	50%	13	67%	14
Group 4	0%	6	0%	7	17%	12	33%	13	67%	15

1. rate = union rate; 2. score = total union score

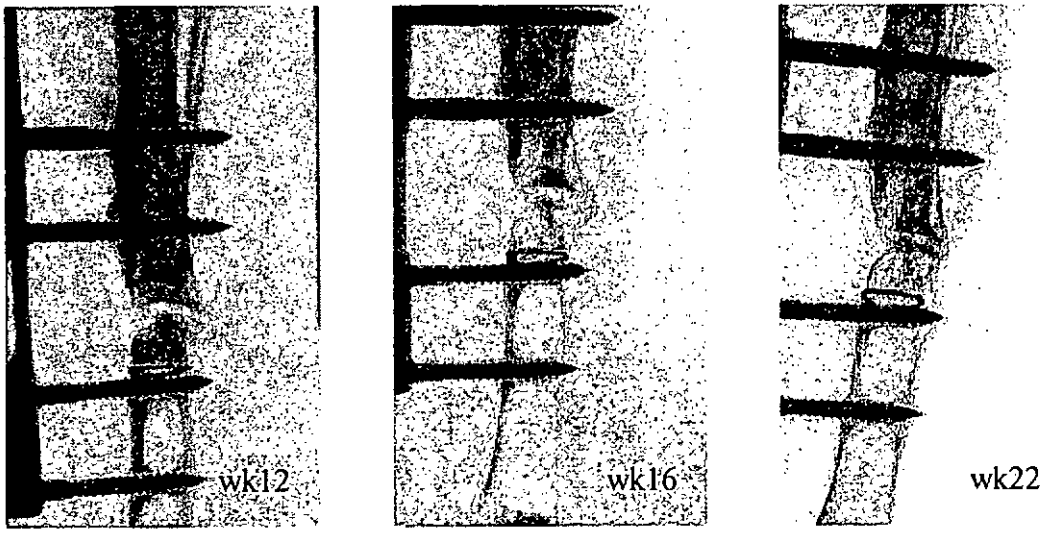

Fig 3.1b. Serial radiographs of SW72 (control group) taken at post-op week 12, 16 and 22. Persistent fracture gap and sclerotic bone ends remained unchanged over time.

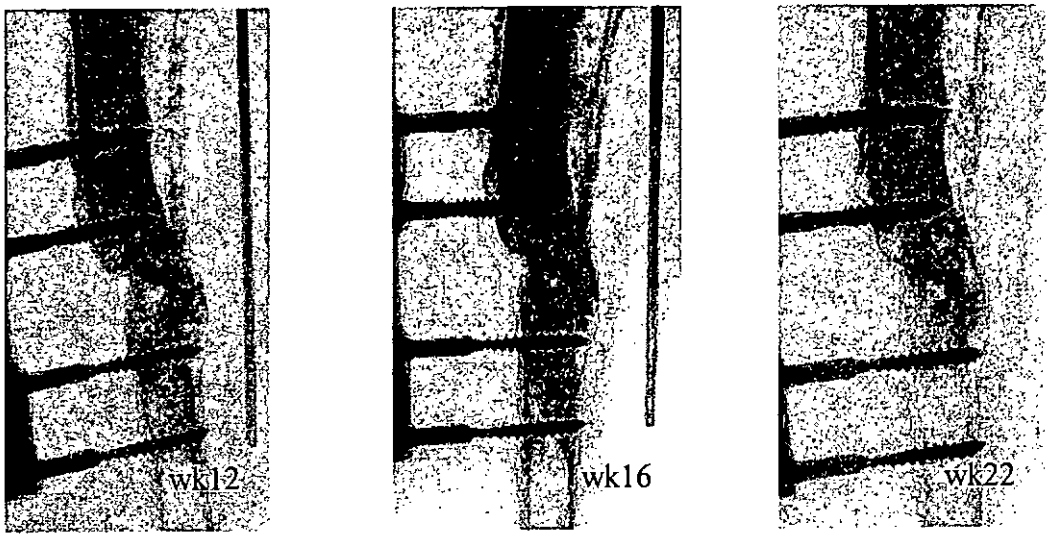

Fig 3.1c. Serial radiographs of SW29 (ESW group) taken at post-op week 12, 16 and 22. Show new mineralization within the gap after treatment, and gradual bridging across the non-union gap.

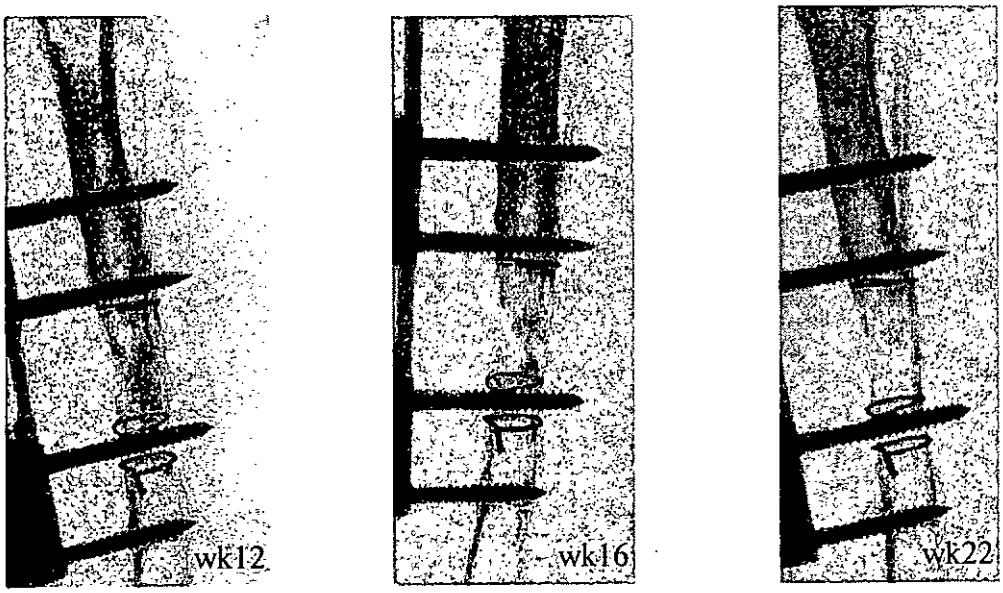

Fig 3.1d. Serial radiographs of SW71 (LIPU group) taken at post-op week 12, 16 and 22. Show a gradual decrease in bone density and bony remodeling at the non-union site.

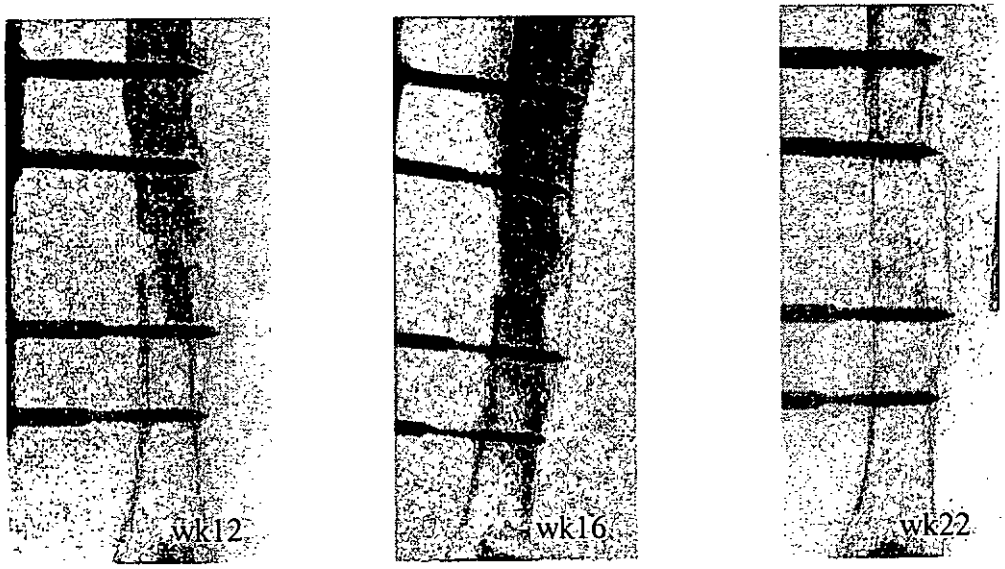

Fig 3.1e. Serial radiographs of SW35 (combined group) taken at post-op week 12, 16 and 22. Pattern similar to that of the LIPU sample with bony remodeling at the non-union site over time.

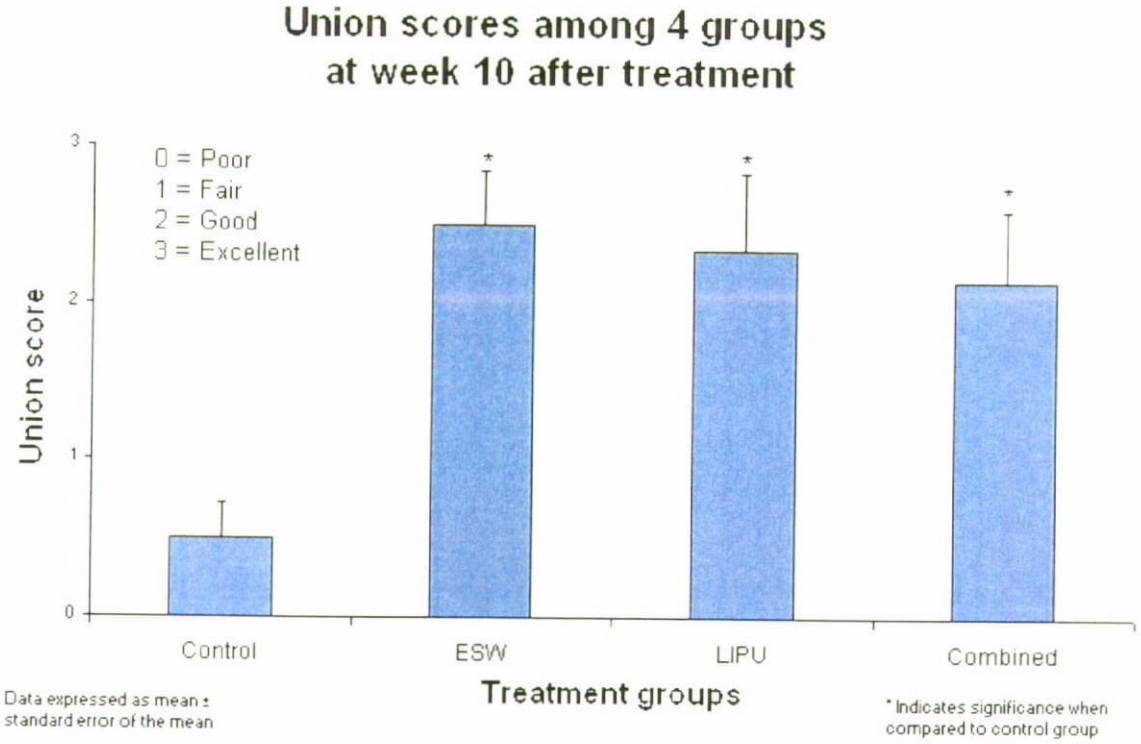

Fig 3.1f. Union Scores of the 4 groups at week 10 after treatment. (* $p<0.05$)

3.2. Peripheral quantitative computerized tomography (pQCT)

pQCT measurement was performed on 22 of the 24 animals. Two rabbits were excluded because the machine was not available at the time of the rabbits were euthanized. As a result, the animal distribution for the purposes of the pQCT analysis was as follows: 6 animals in the control group, 4 animals in the ESW group, 6 animals in the LIPU group, and 6 animals in the combined treatment group.

Table 3.2a. Grouping of rabbits for pQCT measurement

Group Description	**Rabbit Code (SW)**
I. Control	46, 51, 69, 72, 73, 76
II. ESW treatment	29, 41, 58, 64
III. LIPU treatment	48, 53, 54, 71, 74, 75
IV. Combined treatment	35, 44, 59, 65, 66, 68

The bone mineral content (BMC) value of each slice for the pQCT scanning was calculated using the following formula:

BMC = volumetric BMD × volume of bone (area × 1 mm thick slice)

The area was auto-detected by the analysis software with the threshold value set at 280 mg/cm^3. The threshold value was selected because it corresponded to the lower BMD of both cortical and trabecular bone. This value was fixed for all pQCT measurements.

The measured mean BMC value for the control group, ESW group, LIPU group and combined treatment group were 382mg ± 2.8, 455mg ± 12.8, 344mg ± 8.6 and 337mg ± 9.4 respectively (data expressed by mean gram ± standard error of mean). One-way ANOVA showed no significant difference in BMC among the four groups. The graphical presentation of the foregoing is shown in figure 3.2a.

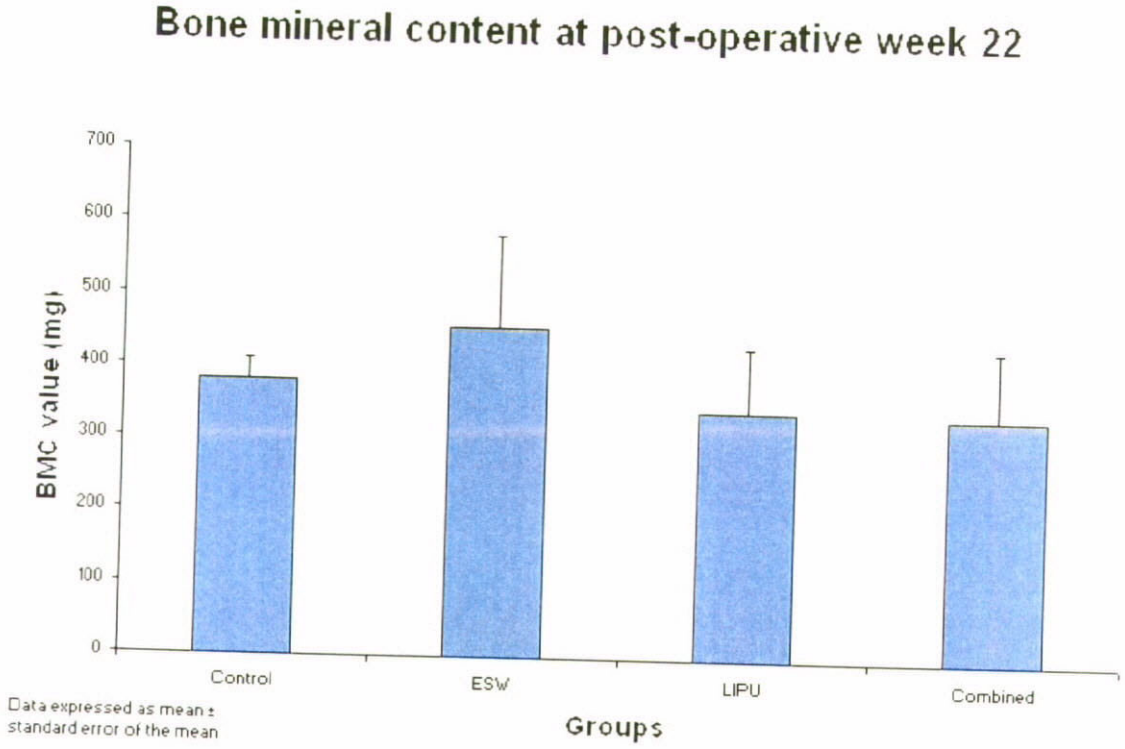

Fig 3.2a. BMC at fracture site measured by pQCT. No significant result was detected in this analysis

3.3. 3D microcomputerized tomography

The 3D micro-CT reconstructions of the non-union sites 10 weeks after the different treatments are illustrated in figure 3.3a.

Group I: Control group

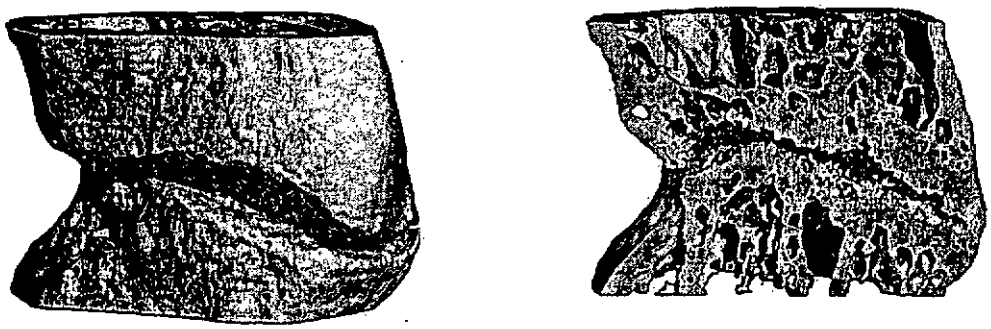

Group II: ESW group

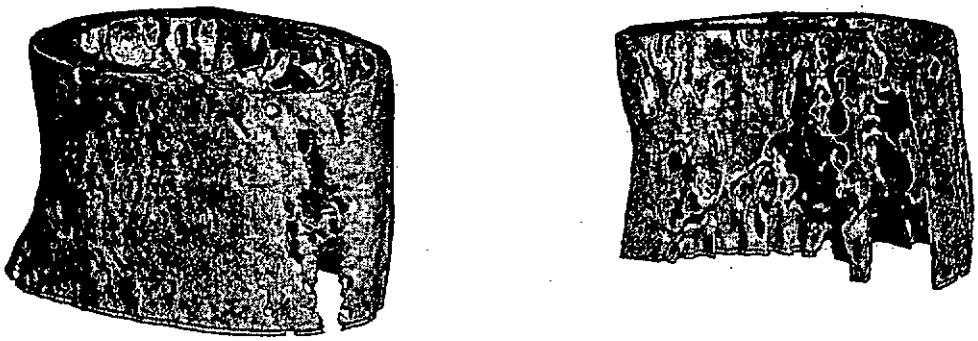

Fig 3.3a. 3D μCT reconstructions of cortical (left side) and trabecular (right side) structures. The trabecular structure shown was cut at the vertical mid-point of the cortical picture. (Resolution: 36μm)

Fig 3.3a. (Cont'd)

Group III: LIPU group

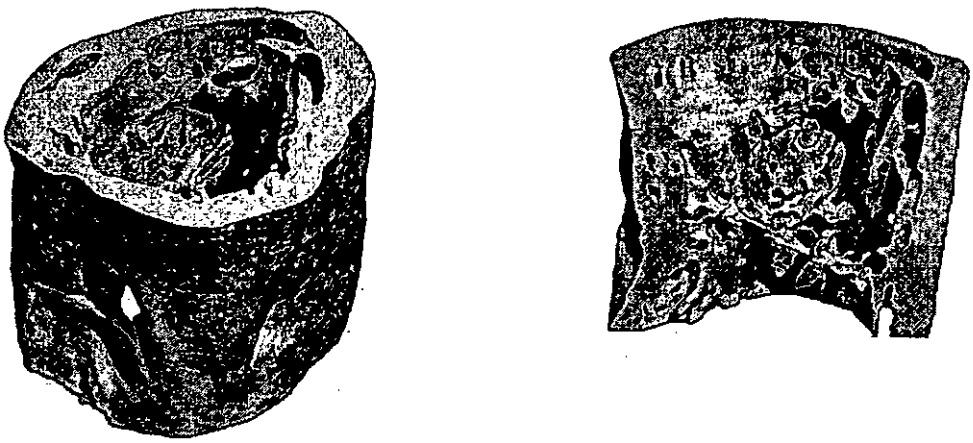

Group IV: Combined group

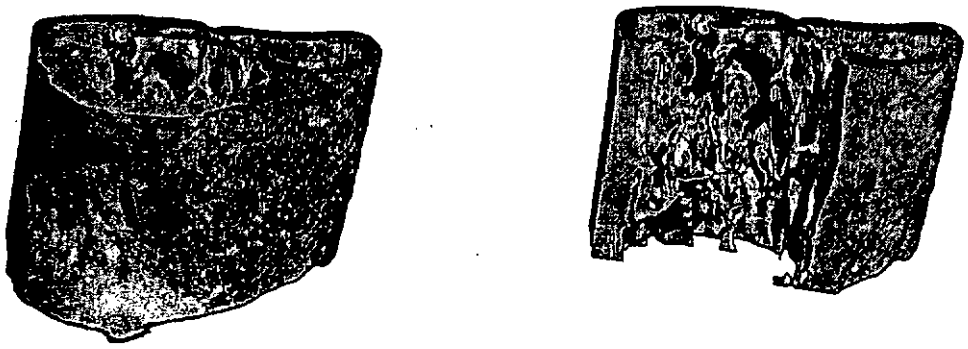

The samples from the control group showed a clear non-union gap. The bone ends were sclerotic and the intramedullary canals were sealed by sclerotic trabecular bone.

The successful union samples of the treatment groups showed bony bridging. The cortex in the two groups with LIPU treatment was thicker than that in the ESW group.

Under fluorescence microscopy, the temporal and spatial pattern of new bone formation was demonstrated by sequential vital labeling. The new mineralization of the first 4 weeks after treatment was labeled by green fluorescent dye and from the 4th week onward by red fluorescent dye. Figure 3.4a shows a histomorphometric measurement of new bone formation in the non-union gap from a longitudinal section.

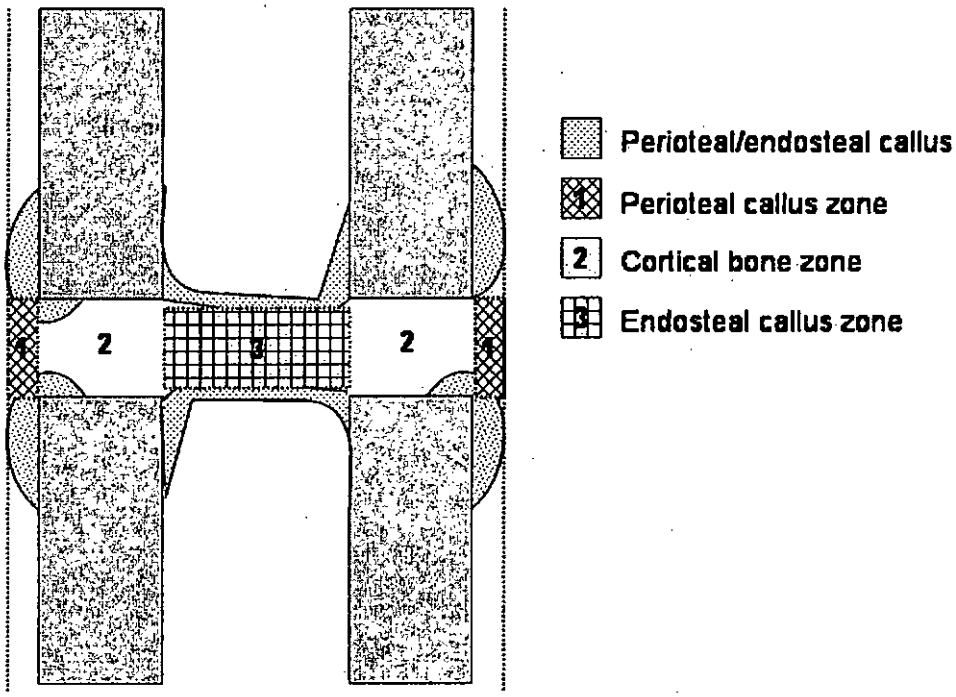

Fig 3.4a. Diagram shows the histomorphometric measurement of new bone formation in the nonunion gap from a longitudinal section.

The fluorescent picture of one representative ESW-treated rabbit (SW29) was used for descriptive histology. It shows the woven bone in green across the gap. Mineralization began in the first 2 weeks after treatment, and persisted up to 10 weeks after treatment. The woven bone in the intramedullary canals mainly formed between the 4th and 10th weeks after ESW treatment. Remodeling of the transected cortices was observed during the first 2 weeks and became extensive from the 4th week onwards (Fig 3.4c).

From one representative picture of the LIPU sample (SW48), the gap was bridged with less green woven bone than in the ESW sample, indicating that mineralization began later than the sample which had undergone ESW treatment. Remodeling of cortices was observed mainly at the 4th week of treatment (Fig. 3.4d).

From one representative picture of the combined treatment sample (SW44), the bridging of the gap was found to be almost equally divided between green and red woven bone. This demonstrates that the bone bridging did not mainly occur in the first 2 weeks as in the ESW sample. The lining of the external callus was found at the outer region of the fracture gap. Remodeling of the cortices was observed at the 4th week of daily LIPU treatment (Fig 3.4e).

The picture of the control group sample (SW46) shows that the fracture gap was persistent and sclerotic bone ends remained at the cortices (Fig 3.4b).

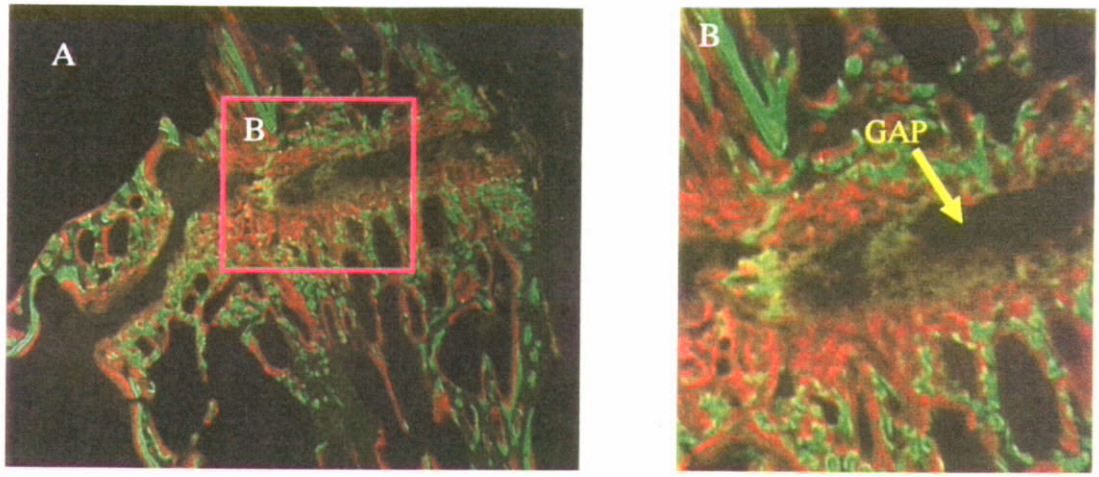

Fig 3.4b. Fluorescent microscopy of control group sample. **GAP**: non-union gap
A: overview of the gap, with magnification was set at 1.6x.
B: computer enlargement of the small region in picture A.

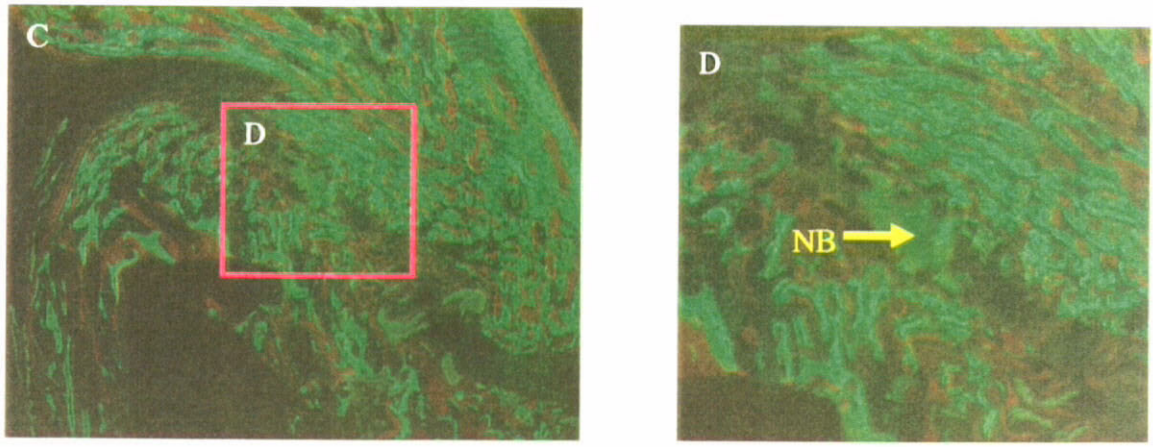

Fig 3.4c. Fluorescent microscopy of ESW group sample. **NB**: site of new bone formation.
C: overview of the treatment site, with magnification was set at 1.6x.
D: computer enlargement of the small region in picture C.

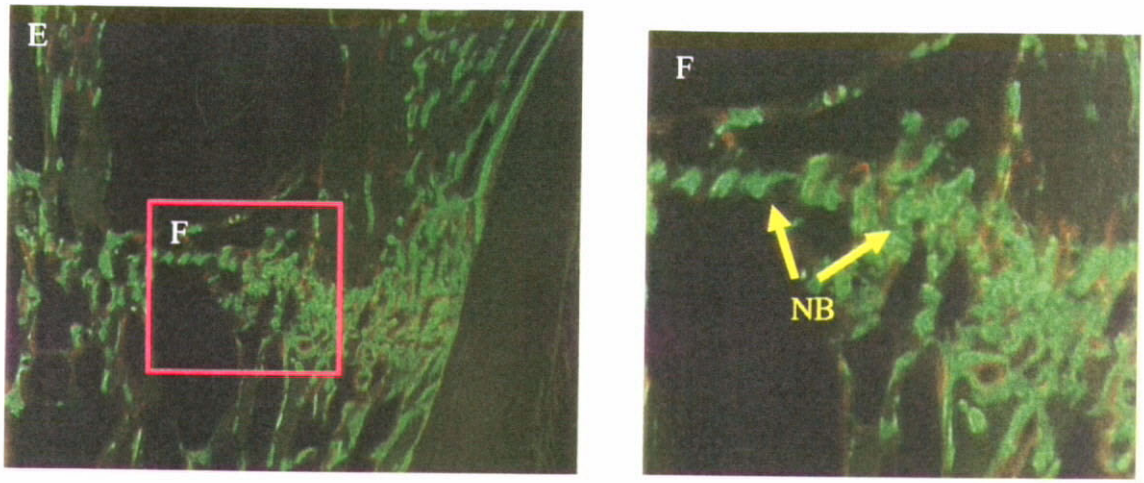

Fig 3.4d. Fluorescent microscopy of LIPU group sample. **NB**: site of new bone formation.
E: overview of the treatment site, with magnification was set at 1.6x.
F: computer enlargement of the small region in picture E.

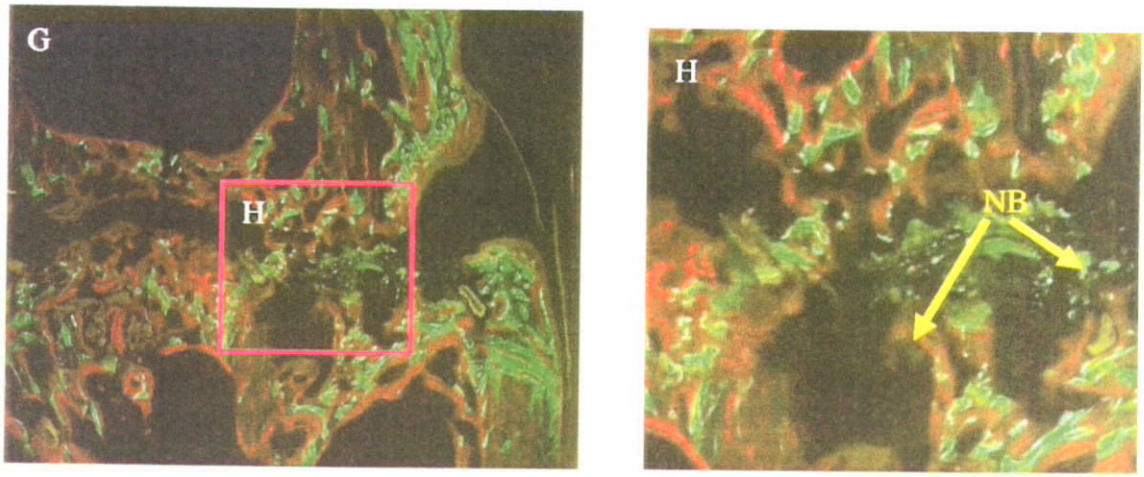

Fig 3.4e. Fluorescent microscopy of combined treatment group sample.
NB: site of new bone formation.
G: overview of the treatment site, with magnification was set at 1.6x.
H: computer enlargement of the small region in picture G.

Three samples in each group were used for histomorphometric analysis of polychrome sequential labeling. The total sample size was set at 12 in this analysis because the fluorescence in some of the samples had faded and only one color was visible. Furthermore, as decalcified tissue processing was performed on one sample in each group these samples could not be included in the analysis.

Using the ImageJ software, the red and green colors were separated and the green and red distribution percentages were calculated. The measured mean value of the green in the control group, the ESW group, the LIPU group and the combined group was 47.6%, 54.3%, 53% and 50.7% respectively. The measured mean value of the red in the control group, the ESW group, the LIPU group and the combined group was 52.3%, 45.7%, 47% and 49.3% respectively. No significant difference was observed in this analysis. The graphical representation is illustrated in the following figure (Fig 3.4f).

The color distribution results suggest that the ESW-treated tibiae had an earlier regeneration of bone beginning within two weeks after treatment, as more green dye was observed in this group than in either of the other treatment groups. Daily LIPU treated tibiae had a slower onset of mineralization than ESW as indicated by the lower green color content and higher red color content in the samples, the latter representing mineralization from the 4th week onwards after treatment. The tibiae subjected to the combined treatment showed a relative average of new mineralization across the 10 weeks

of treatment. However the differences were not significant and a larger sample size would be required for a better representation of this result.

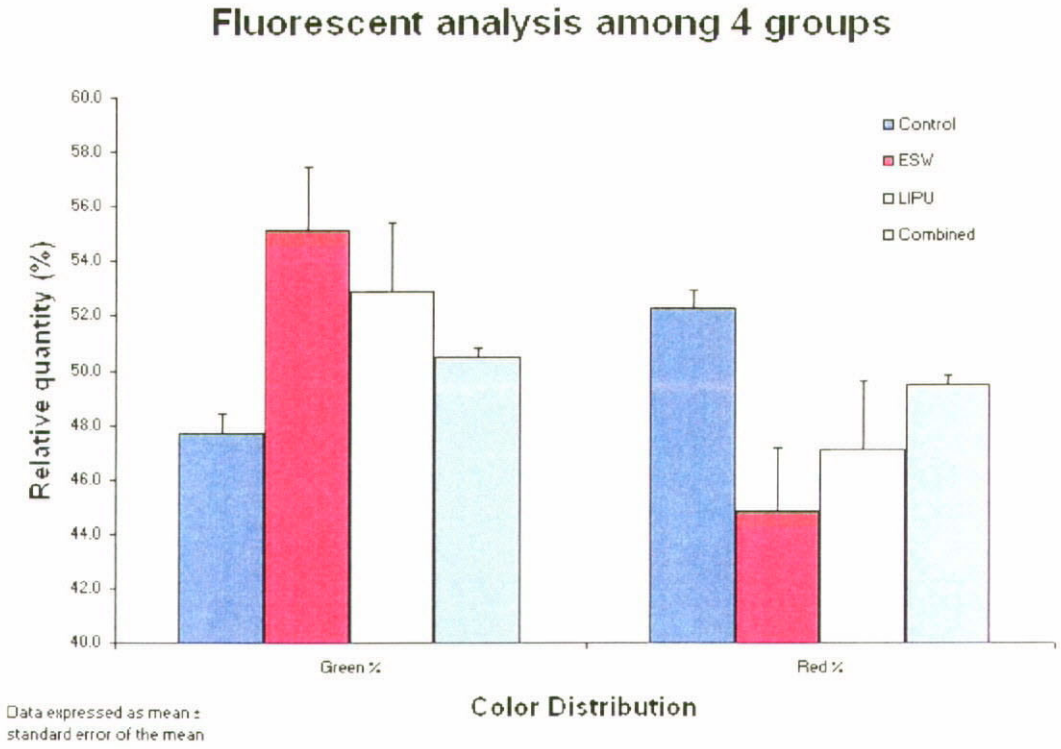

Fig 3.4f. Fluorescent analysis of the 4 groups. The ESW sample had an earlier regeneration of bone beginning within the first two weeks, with more green dye (54.3%) than the LIPU sample (53%). The LIPU sample had a higher red dye content (47%) than the ESW sample (45.7%), which suggests a slower onset of mineralization with the LIPU treatment. Combined treatment showed a relative average of new mineralization with a similar green dye (50.7%) and red dye (49.3%) average across the 10 weeks of treatment. No significant difference was detected.

3.5. Light Microscopy

The density of the osteocytes in the newly formed bone after the different treatments was measured from sections with H&E staining under light microscopy. For the method of counting see the section on methodology. The histological pictures are shown in figures 3.5a, 3.5b and 3.5c.

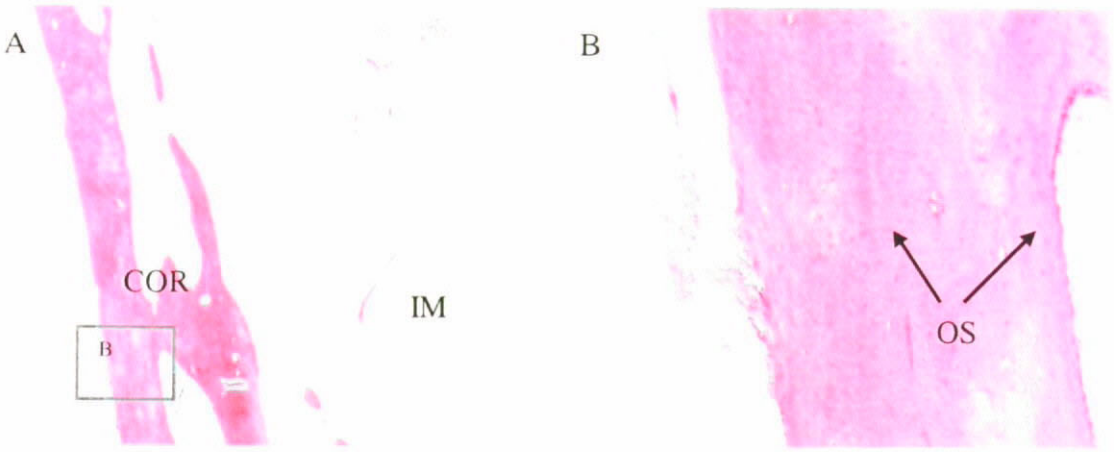

Fig 3.5a. ESW treatment sample with H&E staining. **OS**: osteocytes; **COR**: cortical bone; **IM**: intramedullary canal

A: Histological characterization of treatment site (x1.6).
B: Illustration of density of osteocytes (x10).

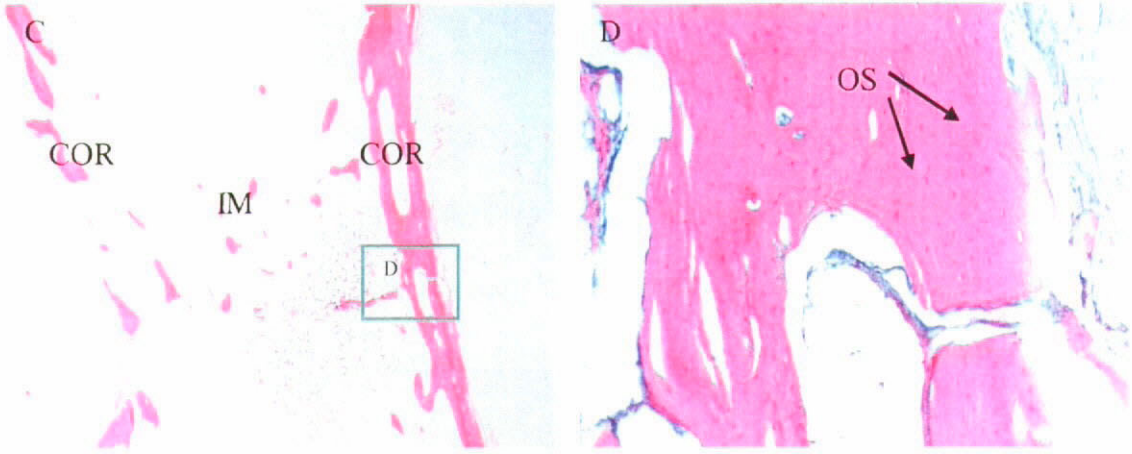

Fig 3.5b. LIPU treatment sample with H&E staining. **OS**: osteocytes; **COR**: cortical bone; **IM**: intramedullary canal

C: Histological characterization of treatment site (x1.6).
D: Illustration of the density of osteocytes (x10).

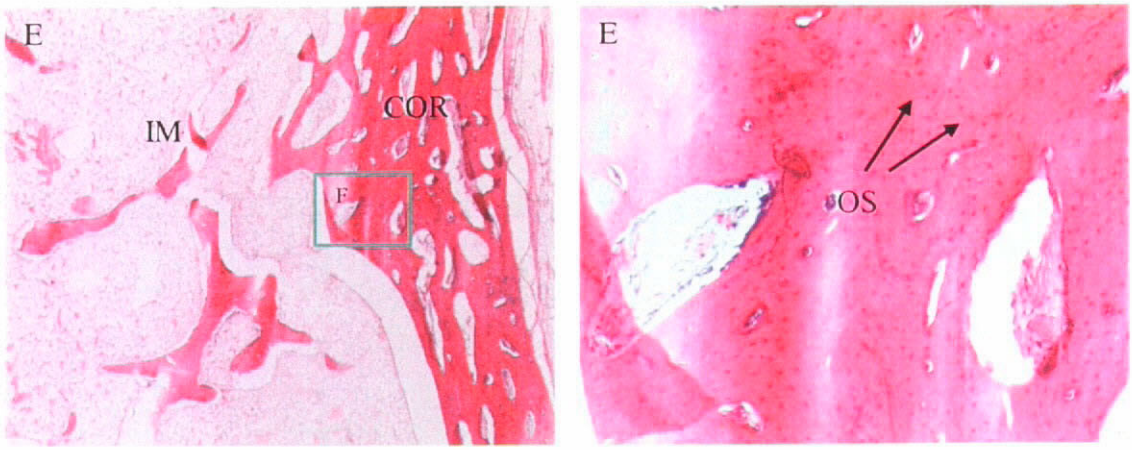

Fig 3.5c. Combined treatment sample with H&E staining. **OS**: osteocytes; **COR**: cortical bone; **IM**: intramedullary canal

E: Histological characterization of treatment site (x1.6).
F: Illustration of the density of osteocytes (x10).

By counting the number of cells in 3 different fixed 400 × 400 pixel regions of the photos taken at 10x magnification, the average cell number in the combined treatment sample was the highest (56.7±1.2) whereas that of the ESW treatment sample (33.7±0.9) and that of the LIPU treatment sample (34.7±3.3) were similar to one another but lower than that of the combined treatment group. However, as only one sample was included in each group for this study, a larger sample size would be required to perform a further statistical analysis to verify this result.

Chapter 4: Discussion

The objectives of the study were primarily to compare the success rate, healing quality and healing time of a bony non-union associated with such biophysical interventions as isolated ESW and LIPU therapies and combined ESW and LIPU therapy. In addition, the pattern of induced healing of non-union has been investigated with x-ray and fluorescent analysis.

The healing of fracture non-unions was investigated by using the rabbit tibia non-union model. It was shown that all three interventions can induce osteogenesis at the non-union site and result in bony bridging of the non-union.

4.1. Effectiveness of ESW treatment

The effectiveness of ESW treatment in healing fracture non-unions is reflected by the success rate of bony bridging and the union score. The complete union rate was 67% at 10 weeks for all 3 interventions, significantly higher than the union rate (0%) of the controls. The significant higher union rate suggests that ESW is effective in restoring the bony continuity of fracture non-unions. The success rate of ESW treatment in this animal experiment is comparable with that of human trials, in a range of 72-80% [45, 49, 59]. The union score and the callus index reflect the quality of ESW promoted bony union. Gardner et al conducted a study correlating callus index with the mechanical strength of the callus [18]. It has been suggested that full loading is allowed when the diameter of the callus reaches 75% of the diameter of the bone shaft. Although no mechanical tests were performed in the study due to the limited budget and time, the fact that the value of the callus index was higher than 75% of the diameter of the bone shaft would indirectly suggest the sufficient mechanical strength of the ESW-promoted bony bridging.

4.2. Parameters of ESW treatment

The effectiveness of ESW treatment is highly dependent on the energy level and other application parameters. Low energy and medium energy ESW treatments are non-destructive and suitable for promoting healing [46]. High energy ESW treatment causes destructive changes at the treatment site, especially to tissues with a high acoustic impedance such as bone [46]. Accordingly, ESW at the appropriate energy level can initiate ossification of the non-union condition without causing harmful destruction of bone.

In previous studies, experiments were conducted on the normal intact bone of different animals to observe the dose-dependent reactions of cortical and trabecular bones to ESW treatment. Kaulesar used normal rabbit femur and tibia to test the immediate effect of direct application of ESW treatment to the cortical surface at different dosages [27]. His results showed cortical damage after the trial application of ESW using 1,000 shocks at an energy level of 0.54 mJ/mm^2. With 10,000 shocks at an energy level of 0.6 mJ/mm^2, complete fracture of the bone was found at the treatment site. He concluded that there was "decortication" and "fragmentation" in the cortical bone caused by the effect of ESW treatment using 1,000 shocks at energy levels of 0.54 mJ/mm^2 or above [27]. A later report by Delius supports this finding [8]. He subjected intact rabbit femur to ESW treatment at a setting of 1,500 shocks of 27.5 kV (about 0.4 mJ/mm^2), i.e. an increased number of shocks at a lower energy level. "Periosteal detachment" and "subcutaneous haemorrhage" were found immediately after ESW treatment [8]. Based on the outcomes

of these experiments, the ideal parameters to induce healing of non-unions using ESW treatment have been determined to be 1,000 shocks at 0.4 to 0.54 mJ/mm^2 [8, 27]. The present study and an animal experiment also using the non-union model reported by Johannes [26] offer further proof that these parameter settings are effective in healing non-unions.

4.3. Pattern of ESW promoted healing of non-union

In our study, several outcome measures were used to determine the pathway by which ESW promoted osteogenesis in the non-union gap. The measurements were taken by radiography, microCT, fluorescent microscopy and light microscopy. The findings suggest gradual bone formation in the non-union gap after ESW treatment, followed finally by a bridging of the gap with newly formed bone. This pattern is quite similar to that demonstrated in the experiment done by Johannes using the dog leg non-union model [26]. He applied the ESW treatment to the non-union site using 1,000 shocks at an energy level of 0.54 mJ/mm^2. His results showed that there were no radiological signs of change immediately after the ESW treatment. The first sign of radiographic change was discovered at week 6 after treatment of his dogs and bony union was achieved at week 12 after treatment [26]. Several clinical papers also support the gradual changes after ESW application [45, 49, 59]. Serial radiographs showed minimal or lack of observable callus formation or bony destruction immediately after ESW treatment. The gap distance gradually decreased over months and was finally bridged. We believe that we have reproduced this pattern of bridging following ESW treatment, which is a gradual process ultimately ending with a bridging condition some weeks later.

In our study, the healing process was found to be different from that after surgical treatment in that it involved very little or no external callus formation. ESW treatment resulted in early bone bridging at the center of the gap at around post-op weeks 12-14, followed by a gradual increase in the remodeling process starting from week 16 onwards,

as shown by polychrome sequential labeling. Our study demonstrates that the bony reaction was sustained for around 8 to 10 weeks after ESW treatment. This finding is consistent with the results of previous animal experiments observing bone formation after the application of ESW to intact bone. Polychrome sequential labeling was used by Delius to observe bone formation initiated by ESW treatment in the distal femur of rabbits [8]. Four fluorescent dyes were used in his study at eight-day intervals after ESW treatment. He found endosteal new bone on the endosteal surface during the 4th week after ESW treatment, and bone cortex up to twice the normal thickness, stained with the later three fluorescent colors, which suggested that cortical thickening began during the second week after ESW treatment [8]. This pattern of new bone formation is quite similar to the healing pattern found in our study, with the fluorescent green (54.3%) and some fluorescent red (45.7%) found in the bridging of the gap after ESW treatment.

The molecular mechanism of ESW-promoted bone healing is still not clear. Wang performed an experiment on femoral defects in rats to investigate the molecular mechanism [60]. He applied 500 shocks of ESW at an energy level of 0.16 mJ/mm^2. The samples were harvested after 1, 2, 4 and 8 weeks and immunohistochenistry was used to observe the molecular events in the bone following ESW treatment. He found that ESW treatment increase bone morphogenetic protein activity. Another study by Martini tested the dose-dependent effect of ESW on cultured human osteoblasts [33]. Osteoblasts were treated with ESW using 500 and 1,000 pulses at 0.15, 0.31 and 0.4 mJ/mm^2 and then observed for 48 hours. His results showed that the number of osteoblasts significantly increased, with new bone matrix deposition, after treatment with ESW at 0.15 and 0.31

mJ/mm^2 energy levels, while the number of cells decreased in the 0.4 mJ/mm^2 group, indicating that ESW had a destructive effect on osteoblasts at this higher energy level.

In our study, the cartilage and fibrous tissue in the gap was replaced by the newly formed bone after ESW treatment. This finding suggests that bone bridging was triggered by endochondral ossification of the cartilage inside the gap, as shown by polychrome labeling. Our study suggests ESW initiates endochondral bone formation inside the gap first, followed by gradual remodeling of the proximal and distal cortices and intramedullary bone formation. The pattern of bone formation is different from the callus formation which occurs in the normal healing process of fresh fractures.

4.4. Effectiveness of LIPU treatment

In our study, the union rate following LIPU treatment (67%) was similar to that resulting from ESW treatment and significantly higher than that in the control group. The result is in line with the findings of previous animal and human studies suggesting that LIPU is effective in healing fracture non-unions [11, 34, 37, 39, 41, 53].

However, the union rate following LIPU treatment in our study was lower than the reported clinical union rate, which ranges from 86% to 100% [34, 37, 39]. The reason for the lower union rate may be a result of the relatively short treatment period. According to clinical studies, the healing of non-unions takes on average 3.4 months after ESW treatment and around 5 months after LIPU treatment. With polychrome sequential labeling we observed that by the end of the experiment (10 weeks after treatment) bone formation at the non-union gap had ceased (Fig. 3.4c) in the ESW treated animals while it was still active in the LIPU treated animals (Fig. 3.4d). This would indicate that the success rate in the LIPU group could increase further.

4.5. Pattern of LIPU promoted healing of non-union

A number of previous studies investigated the effect and mechanism of LIPU-promoted bone healing. Duarte tested the effect of LIPU on rabbit fibular osteotomy. He found a significantly faster growth of callus in the osteotomy gap resulting from LIPU treatment [11]. Parvizi applied LIPU to cultured rat chondrocytes and observed that endochondral ossification could be promoted by an increased aggrecan messenger RNA level and increased proteoglycan synthesis [41]. Takikawa investigated the healing mechanism of LIPU in a rat tibia non-union model, and concluded that the LIPU-generated mechanical force on the fibrous tissue in the gap could lead to differentiation of chrondrocytes and resulted in endochondral ossification [54]. Tis applied LIPU to rabbit tibia distraction osteogenesis, and concluded that LIPU could augment the consolidation of distraction osteogenesis [53]. These studies suggest that LIPU can accelerate bone healing in normal fractures, and to some extent, initiate bone formation in non-union conditions by stimulating the fibrous tissue inside the gap. This is consistent with our finding that LIPU promoted non-union healing.

The radiographs in our study showed that the healing pattern in LIPU-promoted healing of non-unions was characterized by gradual mineralization at the non-union site with the density of the central region gradually decreasing up to 10 weeks after treatment. Takikawa et al applied LIPU treatment to rat tibia non-unions [54]. They created the tibia non-union model by cutting the bone at the diaphysis and inserting muscle fragments into the gap. After the non-union condition was established, they applied LIPU to the non-

union daily for 6 weeks. Their results showed a 50% success rate of complete bony bridging. The fracture gap showed evidence of both intramembranous and endochondral bone formation, with the fracture line still present at 4 weeks after treatment. Diminution of the fracture line and decreased fracture callus were observed at 6 weeks after treatment. One of the clinical reports also demonstrated that LIPU-promoted healing of non-unions occurred through the gradual ossification of tissue in the non-union gap. The radiographs in a case study on one congential pseudoarthrosis patient treated with LIPU showed that the non-union site only had a small amount of callus at 6 months after treatment, and that the gap had gradually been bridged after 12 months of treatment [39].

4.6. Effectiveness of combined treatment

The union rate following combined ESW and LIPU treatment was significantly higher than that in the control group, suggesting that combined treatment is effective in healing non-unions. However, the union rate in this group was no higher than that in the ESW group or the LIPU group. The result failed to support the hypothesis that a combined treatment was superior to either treatment alone.

The role of ESW is to initiate the osteogenesis process in the non-union gap while that of LIPU is to accelerate and sustain the healing process. Accordingly we had postulated that a combined application of ESW and LIPU might have an effect superior to that of either treatment alone. However, we found that the healing pattern and final outcome after the combined treatment were not different from those after LIPU treatment alone.

The healing effect of ESW takes several weeks to occur, from the period of delivery of acoustic energy to the hard tissue until the effect of new bone formation in the gap. However, in our experiment design, we applied LIPU immediately on the second day after ESW treatment. This may have disrupted the "ongoing" effect of ESW, or inhibited the healing process by ESW in the first 2 to 4 weeks after treatment. In our preliminary findings, we were unable to detect any changes inside the gap within the first two weeks. Histological study at these time points could possibly help in exploring this issue further.

4.7. Clinical Significance

ESW treatment is a new and powerful tool in the healing of non-unions. Its effectiveness was investigated in this study. With the advantages of non-invasiveness and the requirement of fewer treatment sessions, it is a good choice in a clinical situation if the clinical setting can afford the cost of purchasing such a machine.

LIPU treatment is a non-operative treatment for the healing of non-unions which is backed by a larger quantity of clinical evidence. It is widely used because the cost is low, the machine is small and portable and, unlike ESW, anesthesia is not required. The only disadvantage may be that it requires a longer course of treatment.

In our study, we were unable to demonstrate any significant superior effect of a combined treatment as compared to individual treatments with either ESW or LIPU. However, the combination of ESW and LIPU treatment in the study is only a starting point at this stage. More research is required to prove the effectiveness of this treatment modality.

4.8. Limitations of the study

Because of the limited time and rabbit living space, we were unable to use a larger sample size in the experiment. As a result, the rabbits were all euthanized at the same time point 22 weeks post-operatively. Although the progression of histological changes could be intimated somewhat by the examination of the fluorescent dye staining patterns, information on the synthetic or mitotic activity of the cellular elements of the callus and surrounding tissues could not be provided by this study. A design using sequential takedowns of the animals would better show the progression in healing.

Bibliography

1. Aronson J, Shen XC, Gao G et al.: Sustained proliferation accompanies distraction osteogenesis in the rat. J Orthop Res. 1997;15:563-9

2. Bahn S, Mehara AK: Percutanous bone grafting for nonunion and delayed union of fractures of the tibial shaft. Int Orthop. 1993;17:310-2

3. Barou O, Valentin D, Vico L, Tirode C et al.: High-resolution three-dimensional micro-computed tomography detects bone loss and changes in trabecular architecture early. Investigative Radiology. 2002;37:40-6

4. Biedermann R, Martin A, Handle G, Auckenthaler T, Bach C, Krismer M: Extracorporeal shock waves in the treatment of nonunions. J Trauma. 2003;54;936-42

5. Birnbaum K, Wirtz DC, Siebert CH, Heller KD: Use of extracorporeal shock-wave therapy (ESWT) in the treatment of non-unions. Arch Orthop Trauma Surg. 2002; 122:324-30

6. Brownlow HC, Simpson AHRW: Metabolic activity of a new atrophic nonunion model in rabbits. J Ortho Res. 2000;18:438-42

7. Buckley MJ, Banes AJ, Levin LG et al.: Osteoblasts increase their rate of division and align in response to cyclic, mechanical tension in vitro. Bone Miner Res. 1988;4: 225-36

8. Delius M, Draenert K, Aldiek Y, Draenert Y: Biological effects of shock waves: in vivo effect of high energy pulses on rabbit bone. Ultrasound Med Biol. 1995; 21:1219-1225

9. Delius M, Draenert K, Draenert Y, Boerner M: Effect of extracorporeal shock wave on bone: a review of shock wave experiments and the mechanism of shock wave action. In Siebert W, Buch M (eds): Extracorporeal shock waves in orthopaedics. Springer, 1997

10. Delloye C, Simon P, Nyssen-Behets C, Banse X et al.: Perforations of cortical bone allografts improve their incorporation. Clin Orthop Res. 2002;396:240-7

11. Duarte LR: The stimulation of bone growth by ultrasound. Arch Orthop Trauma Surg. 1983;101:153-9

12. Einhorn TA: Current concepts review: Enhancement of fracture healing. J Bone Joint Surg. 1995;77A:940-56

13. Einhorn TA, Lane JM: Concept of fracture union, delayed union, and nonunion. Clin Orthop. 1998;355S:22-30

14. Einhorn TA: Clinically applied models of bone regeneration in tissue engineering research. Clin Orthop. 1999;367s:59-67

15. Einhorn TA: Problems with delayed and impaired fracture healing remain a challenge to the orthopedic trauma surgeon. J Orthop Trauma. 1997;11:243

16. El-Shazly M, Saleh M, Coulton L et al.: Biological activity in nonunions. J Orthop Trauma. 1999;13:313

17. Forriol F, Solchaga L, Moreno JL, Canadell J: The effect of shockwaves on mature and healing cortical bone. Inter Orthop. 1994;18:325-9

18. Gardner TN, Hardy J, Evan M, Kenwright J: Temporal changes in dynamic inter fragmentary motion and callus formation in fractures. J Biomech. 1997;30:315-21

19. Guo X, Lee KM, Law LP et al.: Recombinant human bone morphogenetic protein-4 (rhBMP-4) enhanced posterior spinal fusion without decortication. J Orthop Res. 2002;20:740-746

20. Hanson PD, Warner C, Kofroth R et al.: Effect of intramedullary polymethymethacrylate and autogenous cancellous bone on healing of frozen segmental allografts. J Orthop Res. 1998;16:285-92

21. Haupt G, Haupt A, Ekkernkamp A, Gerety B, Chvapil M: Influence of shock waves on fracture healing. J Urology. 1992;39:529-32

22. Haupt G: Use of extracorporeal shock waves in the treatment of pseudarthrosis, tendinopathy and other orthopaedic diseases. J Urology. 1997;158:4-11

23. Hayda RA, Brighton CT, Esterhai JL: Pathophysiology of delayed healing. Clin Orthop. 1998;355s:31-40

24. Heckman JD, Ryaby JP, McCabe J, Frey JJ, Kilcoyne RF: Acceleration of tibial fracture healing by non-invasive, low-intensity pulsed ultrasound. J Bone Joint Surg. 1994;76A:26-34

25. Ikeda K, Tomita K, Takayama K: Application of extracorporeal shock wave on Bone: Preliminary Report. J Trauma. 1999;47:946

26. Johannes EJ, Kaulesar SDM, Matura E: High-energy shock waves for the treatment of nonunions: an experiment on dogs. J Surg Res. 1994;57:246-52

27. Kaulesar SDM, Johannes EJ, Pierik EG et al.: The effect of high energy shock waves focused on cortical bone: An in vitro study. J Surg Res. 1993;54:46-51

28. Kristiansen TK, Rayby JP, Frey JJ, Roe LR: Accelerated healing of acute distal radius fractures using specific, low intensity ultrasound. J Bone Joint Surg. 1997;79A:961-73

29. Latterman C, Baltzer AWA, Whalen JD et al.: Establishment and validation of an atrophic non-union model in a rabbit for the use of gene therapy. Trans Int Soc fracture Repair. 1998;6:55-9

30. Leung KS, Qin L, Lap KF, Chan CW: A comparative study of bone to bone repair and bone to tendon healing in patella-patellar tendon complex in rabbits. Clin Biomech. 2002;17:594-602

31. Mak A, Leung KS, Lee KM, Chan CW, Fung KP: Mechanical characterization of regenerated osseous tissue during callotasis and its related biological phenomenon. Life Sci. 2000;66:327-36

32. Marsh D: Concepts of fracture union, delayed union, and nonunion. Clin Orthop. 1995;355S:S22-S30

33. Martini L, Giavaresi G, Fini M, Torricelli P, Pretto M, Schaden W, Giardino R: Effect of extracorporeal shock wave therapy on osteoblastlike cells. Clin Orthop. 2003;413:269-80

34. Mayr E, Frankel V, Rueter A: Ultrasound – an alternative healing method for nonunion? Arch Orthop Trauma Surg. 2000;120:1-8

35. Muschler GF, Nitto H, Matsukura Y et al.: Spine fusion using cell matrix composites enriched in bone marrow-derived cells. Clin Orthop Res. 2003;407:102-18

36. Naruse K, Miyauchi A, Itoman M, Mikuni-Takagaki Y: Distinct anabolic response of osteoblast to low-intensity pulsed ultrasound. J Bone Min Res. 2003;18:360-9

37. Nolte PA, Krans A, Patka P, Janssen IMC, Pyaby JP, Albers GHR: Low-intersity pulsed ultrasound in the treatment of nonunions. J Trauma. 2001;51:693-703

38. Ogden JA, Anna TK, Schultheiss R: Principles of shock wave therapy. Clin Orthop. 2001;387:8-17

39. Okada J, Miyakoshi N, Takahashi S, Ishigaki S, Nishida J, Itoi E: Congenital pseudoarthrosis of the tibia trated with low-intensity pulsed ultrasound stimulation (LIPUS). Ultrasound Med Bio. 2003;29:1061-4

40. Oni OOA: A non-union model of the rabbit tibial diaphysis. Injury. 1995;26:619-22

41. Parvizi J Wu CC, Lewallen DG, Greenleaf JF, Bolander ME: Low intensity ultrasound stimulates proteoglycan synthesis in rat chondrocytes by increasing aggrecan gene expression. J Orthop Res. 1999;17:488-94

42. Pienkowski D, Pollack SR, Brighton CT, Griffith NJ: Low-power electromagnetic stimulation of osteotomized rabbit fibulae. A randomized, blinded study. J Bone Joint Surg. 1994;76A:489-501

43. Qin L, Leung KS, Chan CW, Fu LK, Rosier R: Enlargement of remaining patella after partial patellectomy in rabbits. Med Sci Sports Exerc. 1999;31(4):502-6

44. Robert RK, Frank PM, Thomas WSG, Theodore M: The lithotripter and its potential use in the revision of total hip arthroplasty. Clin Orthop. 2001;387:4-7

45. Rompe JD, Rosendahl T, Schollner C, Theis C: High-energy extracorporeal shock wave treatment of nonunions. Clin Orthop. 2001;387:102-11

46. Rompe JD: Dose-Dependent Effects of extracorporeal shock waves in a fibular-defect model in rabbits. Shock wave applications in musculoskeletal disorders. New York, Thieme. 2002;23-31

47. Rompe JD: Extracorporeal shock wave application in the treatment of nonunions. Shock wave applications in musculoskeletal disorders. New York, Thieme. 2002;61-70

48. Rosson JW, Simonis RB: Locked nailing for nonunion of the tibia. J Bone Joint Surg. 1992;74B:358-61

49. Schaden W, Fischer A, Sailler A: Extracorporeal shock wave therapy of nonunion or delayed osseous union. Clin Orthop. 2001;387:90-4

50. Shleberger R, Senge T: Non-invasive treatment of long-bone pseudarthrosis by shock waves. Arch Orthop Trauma Surg. 1992;111:224-7

51. Sievanen H, Koskue V, Rauhio A, Kannus P, Heinonen A, Vuori I: Peripheral quantitative computed tomography in human long bones: evaluation of in vitro and in vivo precision. J Bone Min Res. 1998;13:871-82

52. Stock SR, Blackburn D, Gradassi M, Simon H: Bone formation during forelimb regeneration: a microtomography analysis. Developmental Dynamics. 2003;226:410-7

53. Takikawa S, Matsui N, Kokubu T, Tsunoda M, Fujioka H, Mizuno K, Azuma Y: Low-intensity pulsed ultrasound initiates bone healing in rat nonunion fracture model. J Ultrasound Med. 2001;20:197-205

54. Tis JE, Meffert RH, Inoue N, McCarthy EF, Machen MS, McHale KA, Chao EYS: The effect of low intensity pulsed ultrasound applied to rabbit tibiae during the consolidation phase of distraction osteogenesis. J Orthop Res. 2002;20:793-800

55. Uglow MG, Peat RA, Hile MS, Bilston LE, Smith EJ, Little DG: Low-intensity ultrasound stimulation in distraction osteogenesis in rabbits. Clin Orthop. 2003;417:303-12

56. Uslu MM, Bozdogan O, Guney S, Bilgili H, Kaya U, Olcay B, Korkusuz F: The effect of extracorporeal shock wave treatment (ESWT) on bone defects: an experimental study. Bulletin of the Hospital for Joint Diseases. 1999;58:114-8

57. Valchanou VD, Michailov P: High energy shock waves in the treatment of delayed and non-union of fractures. Int Orthop. 1991;15:181-4

58. Vogel J, Hopf C, Eysel P, Rompe JD: Application of extracorporeal shock-waves in the treatment of pseudoarthrosis of the lower extremity. Arch Orthop Trauma Surg. 1997;116: 480-3

59. Wang CJ, Chen HS, Chen CE, Yang KD: Treatment of nonunions of long bone fractures with shock waves. Clin Orthop. 2001;387:95-101

60. Wang FS, Yang KD, Kuo YR et al. Temporal and spatial expression of bone morphogenetic proteins in extracorporeal shock wave-promoted healing of segmental defect. Bone. 2003;32:387-96

61. Warren SB, Brooker AF: Intramedullary nailing of tibial nonunions. Clin Orthop. 1992;285:236-43

62. William EP: Therapeutic modalities for physical therapists. Second edition, McGraw-Hill, New York, London. 2002

63. Wiss DA, Stetson WB: Nonunion of the tibia treated with a reamed intramedullary nail. J Orthop Trauma. 1994;8:189-94

64. Yang KH, Parvizi J, Wang SJ et al.: Exposure to low intensity ultrasound increases in a rat femur fracture model. J Orthop Res. 1996;14:802-9

65. Younger EM, Chapman MW: Morbidity at bone graft donor sites. J Orthop Trauma. 1989;3:192-5

66. Zeng QQ, Jee WSS, Bigornia AE, King JG, Souza SM, Li XJ, Ma YF: Time responses of cancellous and cortical bones to sciatic neurectomy in growing female rats. Bone. 1996;19:13-21

Appendix 1 Operation protocol

A. Materials

- Operation equipments (surgical knife, forceps, air drill, saw, blur)
- Sterile operation pack with cotton wool
- Sterile gloves
- Mask
- Hair shaver
- Operation table (self-designed)
- External fixator with 4 screws
- Diluted hibitane
- 5ml of 2.5% Pentobarbital
- 0.3ml temgesic
- Sterile Saline
- Suture for wound closure

B. Methods

1. The rabbit is anesthesia by 2.5% pentobarbital
2. Shave the hair around right tibia
3. Incision start at 1cm proximal to the tibia tuberosity
4. Incision end at about 2.5cm distal to medial maleolus
5. Incision depth is made until the periosteum exposed

6. Drill the first hole at the medial side of tibia, around 1 cm proximal to tibial tuberosity
7. Insert the first pin
8. Measure the location of fourth pin by the external fixator
9. Mark this location on bone
10. Drill and insert the fourth pin
11. Fit the fixator on that 2 pins
12. Mark the location of the second and third pin on bone
13. Drill and insert the second and third pins
14. Use the saw to cut the bone, at 6mm proximal to second pin and 6mm distal to third pin
15. Take out a 5mm bony defect from the middle of tibia
16. Clear the periosteum and bone marrow between second and third pin
17. Close the incision by suture
18. Intra-muscular injection of 0.3ml temgesic for pain relieving
19. Take care of the rabbit until waked up

Appendix 2 ESW treatment protocol

A. Material

- Shockwave generator (SONOCUR Plus, Siemens, Erlangen, Germany)
- Diluted hibitane
- Coupling gel
- Ketamine and Xylazine
- 3ml Syringe
- Paper towel

B. Method

1. Rabbit is anesthetized by mixture of 0.6ml Ketamine and 0.9ml of Xylazine
2. Tibia is fixed on the operation table
3. Coupling gel is added both on the ESW head and the treatment area
4. Adjust the ESW arm on the treatment area
5. Observe the ultrasound image to locate the focal area
6. Set parameter of ESW as energy level 9, 1000 shocks
7. Start treatment
8. Clean the gel and clean ESW head by diluted hibitane
9. Take care of the rabbit until waked up

Appendix 3 LIPU treatment protocol

A. Material

- Ultrasound generator (SAFHS, Exogen, Inc, West Calwell, NJ, USA)
- Diluted hibitane
- Coupling gel
- Ketamine and Xylazine
- 3ml Syringe
- Paper towel

B. Method

1. Rabbit is anesthetized by mixture of 0.6ml Ketamin and 0.9ml of Xylazine
2. Coupling gel is added both on the ultrasound head and the treatment area
3. Fix the sound head to the treatment area by adhesive tape
4. Turn on machine and start treatment
5. The treatment will automatically stop after 20 minutes
6. Remove the gel and clean LIPU head by paper towel and diluted hibitane
7. Take care of the rabbit until waked up

Appendix 4 Animal recording

Animal Record Form

Rabbit code: SW Age:

Sex: Female Weight:

Group: I / II / III / IV

SW date: US starting date:

Sacrifice date:

Operation date: Last for:

Operation site and comment:

Pins distance (2^{nd} to 3^{rd}):

Radiograph date:
Post-operation

Post-treatment

pQCT measurement:

Fluorescence injection date:

Tissue treatment:

Remarks:

Appendix 5 H & E staining protocol

(Manual book of histology protocols, CUHK)

Chemicals	*Time*
Xylene 1	5 min.
Xylene 2	5 min.
100% Ethanol	3 min.
90% Ethanol	2 min.
70% Ethanol	2 min.
Distilled water	1 min.
Harris' Haematoxylin	12 min.
Distilled water	1 min.
Acid Alcohol	1 sec.
Distilled water	1 min.
Scotts Tap water	3 min.
Distilled water	2 min.
Eosin	5 min.
Distilled water	1 sec.
70% Ethanol	10 sec.
80% Ethanol	10 sec.
90% Ethanol 1	10 sec.
90% Ethanol 2	10 sec.
100% Ethanol 1	3 min.
100% Ethanol 2	5 min.
Xylene 1	3 min.
Xylene 2	5 min.

Appendix 6 MMA embedding protocol

(Manual book of histology protocols, CUHK)

A. Tissue fixation

After harvested, put the sample into 4% phosphate buffered formalin for 2 days.

B. Dehydration and embedding

1. 70% ethanol – 3 days for 2 changes
2. 95% ethanol – 3 days for 2 changes
3. 100% ethanol – 4 days for 3 changes
4. Xylene – 4 days for 3 changes
5. Xylene:UMMA* (in 1:1) I – 1 day
6. Xylene:UMMA (in 1:1) II – 1 day
7. UMMA I – 1 day
8. UMMA II – 1 day
9. UMMA III – 1 day
10. PMMA** – Wait for harden, store at room temperature, vacuum for first 10 mins

* Unpolymerized MMA (UMMA)

** Partially polymerized MMA (PMMA)

Appendix 7 pQCT measurement protocol

A. Equipment

1. XCT 2000 scanner (Stratec, Germany)
2. PC computer with Microsoft windows

B. Set up the system

1. Turn on the RED warning light outside the door
2. Turn on the computer
3. Turn on the pQCT machine (Rotate the red button at back of machine)
4. In windows screen, double click the "Start C-XC7540" icon
5. Enter username and password
6. In the menu, click Measure
7. Click "Select patient" for old subject or "New patient" for new subject
8. Type in the key parameters: Name, ID, Birth Day
9. Press F4 or "Page Down" to Measurement parameter menu
10. Press F6 and choose old reference and killed rabbit tibia
11. Press F4 to start the scout view scan

C. Rabbit tibia sample preparation

1. Place the sample into a plastic bag from 70% ethanol
2. Place the wooden ruler across the x-ray detector
3. Place the tibia on the ruler and set them in the same alignment

D. pQCT measurement procedure

1. Press Enter when tibia position is ready
2. Set the starting position of the detector by pressing "left SHIFT" and "right SHIFT" button
3. Press Enter to start the scout view (SV) scan
4. From SV, choose "Position" and "pos sel" to define the position of measurement lines
5. Press Tab can switch to different measurement lines
6. Choose "Start CT" to start scanning
7. Note the results will be auto-saved after scanning finished

E. Data analysis

1. Choose Analysis and Select patient
2. Enter the patient name in your previous scan
3. Find out the result and enter the analysis program
4. Choose "Analysis" -> "Results" -> "ROI"
5. Choose "New" to define the region of interest (ROI) in that slice
6. If ROI is auto-detected, choose "Name" to rename the region
7. Extract the data by choosing "CALCBD" for cancellous bone density, or "CORTBD" for cortical bone density
8. Repeat to analyze other slices
9. All results can be shown in "Report" or "Survey" when done

Appendix 8 License to conduct experiments

香港特別行政區政府
衞生署
新界東區辦事處
新界沙田上禾輋路一號
沙田政府合署三樓三三一室

THE GOVERNMENT OF THE HONG KONG SPECIAL ADMINISTRATIVE REGION
NEW TERRITORIES (EAST) REGIONAL OFFICE
DEPARTMENT OF HEALTH
ROOM 331, 3/F,
SHATIN GOVERNMENT OFFICES,
NO. 1 SHEUNG WO CHE ROAD,
SHATIN, N.T.

本處檔號 OUR REF.: (191) in DHNTE 007/5 Pt.24

24 July 2002

來函檔號 YOUR REF.:

電 話 TEL.: 2158 5101

傳 真 FAX.: 2603 0523

Hui Chi-cheung Benny
Department of Orthopaedics & Traumatology,
The Chinese University of Hong Kong

Dear Sir/Madam,

Animals (Control of Experiments) Ordinance
Chapter 340

I refer to your application/letter dated 18.4.2002 and forward herewith the following licence(s) issued/duly renewed under the above Ordinance :-

Form 2 : Licence to Conduct Experiments

Your attention is drawn to regulations 4 and 5 of the Animals (Control of Experiments) Regulations, copies of these regulations together with copies of Forms 6 and 7 are enclosed for your convenience. Failure to comply with either regulation 4 or regulation 5 is an offence, each offence punishable by a fine of HK$500 and to imprisonment for 3 months. Conviction of an offence against either regulation 4 or regulation 5 or failure to comply with either regulation may result in your licenece being cancelled.

Please also be reminded that if you wish to continue your experiments after the specified periods as stated on the above licence / endorsements / teaching permit, you should renew them at least one-month before the end-dates. On the other hand, if you have completed or stopped your experiments before the specified periods, you should inform this Office immediately.

Pursuant to the Personal Data (Privacy) Ordinance, a statement of purpose regarding the collection of personal data relating to licence/permit applications under the Animals (Control of Experiments) Ordinance is also attached for your information.

Yours sincerely,

(Dr. T. K. AU)
Community Physician (NTE)
Department of Health

Encl.

TKA/AK/ic

Form 2

Licence to Conduct Experiments

Name : Hui Chi-cheung Benny

Address : Department of Orthopaedics & Traumatology
The Chinese University of Hong Kong

By virtue of section 7 of the Animals (Control of Experiments) Ordinance, Chapter 340, the above-named is hereby licensed to conduct the type of experiment(s), at the place(s) and upon the conditions, hereinafter mentioned.

Type of experiment(s)

Induce non-urion model of rabbit fibia. Surgical procedures would be performed under anaesthesia.

Place(s) where experiment(s) may be conducted

CUHK

Conditions

(1) Such experiment(s) may only be conducted for the following purposes :-

To investigate the shockwave effect on non-urion bone.

(2) This licence is valid until. 23.7.2004

Dated The Twenty-fourth of July 2002

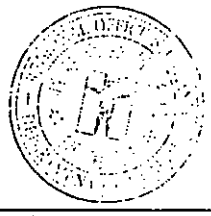

Licensing Authority

We are committed to providing quality client-oriented service

Appendix 9 Ethical Approval

THE HONG KONG
POLYTECHNIC UNIVERSITY
香港理工大學

MEMO

To : Dr Guo Xia, Department of Rehabilitation Sciences

From : Mrs Maureen Boost, Chairman, Animal Subjects Ethics Sub-committee

Ref. : _____ Your Ref. : _____

Tel. No. : Ext. 6391 Date : - 7 APR 2003

Application for Ethical Review for the Use of Animals in Teaching or Research
[Effect of ultrasound for improving tendon healing and prevention of bone loss in disused limbs] (ASESC No. 03/6)
[Combination of extracorporeal shock wave therapy and low intensity ultrasound for inducing healing in a rabbit model] (ASESC No. 03/8)
[Effect of low intensity pulsed ultrasound on PhBMP-4 induced osteogenesis in an spinal fusion model] (ASESC No. 03/9)

Your applications for ethics review for the use of animals in the above projects have been approved for a period of two years from the date of this memo.

You are required to inform the Animal Subjects Ethics Sub-committee if at any time the conditions under which the animals are kept and cared for no longer fully meet the requirements of the Procedures for the Care of Laboratory Animals. If you are keeping animals in the University's animal holding room, you should state the full title of the approved project and the ASESC no. on the cage cards of the cages holding the animals. The members of the Sub-committee may visit the animal holding room unannounced at any reasonable time.

I would like to draw your attention to the University requirement that holders of licences under Cap. 340 must provide the Animal Subjects Ethics Sub-committee with a copy of their licences and a copy of their annual returns to the Licensing Authority. These must be kept up to date for the duration of the above work.

Mrs Maureen Boost
Chairman
Animal Subjects Ethics Sub-committee

c.c. Chairman, DRC (RS)

THE HONG KONG
POLYTECHNIC UNIVERSITY
香港理工大學

MEMO

To : Dr Kwong Shek-chuen, Kevin, Associate Professor, Department of Rehabilitation Sciences

From : Mrs Maureen Boost, Chairman, Animal Subjects Ethics Sub-committee

Ref. : _____ Your Ref. : _____

Tel. No. : Ext. 6391 Date : 11 APR 2001

Application for Ethical Review for the Use of Animals in Teaching or Research [Combination of extra-corporeal shock wave and low intensity ultrasound therapy – an alternative biophysical treatment of fracture non-union]
(ASESC No. 01/5)

Your application for ethics review for the use of animals in the above project has been approved, subject to the condition that analgesia will be applied to the animals at least one week after osteotomy. The approval will be valid for a period of two years from the date of this memo.

You are required to inform the Animal Subjects Ethics Sub-committee if at any time the conditions under which the animals are kept and cared for no longer fully meets the requirements of the Procedures for the Care of Laboratory Animals. If you are keeping animals in the University's animal holding room, you should state the full title of the approved project and the ASESC no. on the cage cards of the cages holding the animals. The members of the Sub-committee may visit the animal holding room unannounced at any reasonable time.

I would like to draw your attention to the University requirement that holders of licences under Cap. 340 must provide the Animal Subjects Ethics Sub-committee with a copy of their licences and a copy of their annual returns to the Licensing Authority. These must be kept up to date for the duration of the above work.

Mrs Maureen Boost
Chairman
Animal Subjects Ethics Sub-committee

c.c. Chairman, DRC (RS)

Conference Papers

Hui CC, Guo X, Chan CW, Kwong KSC, Cheng JCY (2003): Combination of extracorporeal shockwave and low intensity ultrasound for inducing non-union healing in a rabbit model. *The 23rd Hong Kong Orthopedic Association Annual Congress, November 8-9, Hong Kong.*

Hui CC, Guo X, Chan CW, Kwong KSC, Cheng JCY (2003): Extracorporeal Shockwave (ESW) Promoted Healing of Non-union – The pattern and Route of Bridging Callus Formation. *The 23rd Hong Kong Orthopedic Association Annual Congress, November 8-9, Hong Kong.*

Hui CC, Guo X, Chan CW, Kwong KSC, Cheng JCY (2003): Combination of extracorporeal shockwave and low intensity ultrasound for inducing non-union healing in a rabbit model. *Hong Kong student conference in sport medicine, rehabilitation and exercise science, August 31, The Hong Kong Polytechnic University.*

Hui CC, Guo X, Chan CW, Kwong KSC, Cheng JCY (2003): Combination of extracorporeal shockwave and low intensity ultrasound for inducing non-union healing in a rabbit model. *World Congress on Medical Physics and Biomedical Engineering, August 24-29, Sydney, Australia*

Paper submitted to Journal of Orthopaedic Trauma

Hui CC, Guo X, Chan CW, Kwong KSC, Cheng JCY: Extracorporeal shockwave triggers repair of tibial nonunion – an experimental study in rabbits.